 ©2003 Uspekhi Fizicheskikh Nauk, Russian Academy of Sciences

REVIEWS OF TOPICAL PROBLEMS

PACS numbers: 05.40.Ca, **72.70.+m**, 73.50.Td, 85.40.Qx

Nonequilibrium $1/f^{\gamma}$ noise in conducting films and contacts

G P Zhigal'skiĭ

DOI: 10.1070/PU2003v046n05ABEH001244

Contents

1. **Introduction** 449
2. **Concise information on equilibrium flicker noise (EFN)** 450
2.1 EFN model related to fluctuations in the mobility of current carriers scattered by phonons; 2.2 Vacancy model of EFN; 2.3 Temperature dependence of EFN
3. **General information about nonequilibrium flicker noise (NEFN)** 452
3.1 Current-voltage characteristic of a film sample; 3.2 Dependence of nonequilibrium flicker noise PSD on the current
4. **Methods of experimental studies of nonequilibrium flicker fluctuations in conducting films and contacts** 453
4.1 Voltage spectrum of the signal-response in a film sample under harmonic test influence; 4.2 Method for measuring amplitude fluctuation spectra of signal-response harmonics in a sample under harmonic test influence; 4.3 Method for measuring voltage fluctuations of the constant component of the sample's signal-response under pulse test influence
5. **Results of investigations into nonequilibrium flicker noise in conducting films** 455
5.1 Nonequilibrium flicker noise in metal and alloy films due to the generation of excess vacancies; 5.2. Electromigration $1/f^2$ noise; 5.3 NEFN due to heterogeneous inclusions
6. **Nonequilibrium flicker noise in thin-film contacts** 461
6.1 Test samples for separating flicker noise in film contacts measured in direct current; 6.2 Results of investigations into nonequilibrium flicker noise and nonlinearity of CVC in film contacts of resistors
7. **Nonequilibrium flicker noise due to thermodynamic nonequilibrium of film structure and external influences** 465
7.1 NEFN caused by natural aging and annealing of metal films; 7.2 Radiation-induced NEFN in metal films; 7.3 Strain-induced NEFN in conductors
8. **Nondestructive quality control of film conductors, resistors, and contacts by measuring flicker noise** 467
8.1 Forecasting electromigration stability of thin films from $1/f$ noise; 8.2. Quality control of film resistors based on $1/f$ noise; 8.3 New principles of flicker-noise spectroscopy
9. **Conclusions** 469
References 470

Abstract. **Work on nonequilibrium flicker-noise ($1/f^{\gamma}$ noise or NEFN) in conducting films of various materials and in thin-film contacts is reviewed. Experimental methods for studying nonequilibrium flicker fluctuations by separating NEFN from the total noise are suggested. Published results on NEFN in metal and alloy films, Ni/Cr-film and Ta_xN_y-film resistors, and contacts are systematized. It is shown that various kinds of NEFN occur in conducting films. Depending on test conditions, external influences, and the film microstructure, both stationary and non-stationary NEFNs are observed. The use of $1/f^{\gamma}$ noise measurements for nondestructively controlling the quality of thin-film conductors is substantiated. For most of the passive IC components (thin-film conductors, resistive layers, contacts), NEFN makes a much more informative quality indicator than equilibrium flicker-noise.**

G P Zhigal'skiĭ Moscow State Institute of Electronic Technology (Technical University)
124498 Moscow, Zelenograd, Russian Federation
Tel. (7-095) 532 99 24. E-mail: genpal@zelmail.ru

Received 15 June 2002, revised 17 February 2003
Uspekhi Fizicheskikh Nauk **173** (5) 465 – 490 (2003)
Translated by Yu V Morozov; edited by M V Chekhova

1. Introduction

Electrical fluctuations with $1/f^{\gamma}$ spectra (γ is an exponent specifying the shape of the spectrum) have been studied in physical systems since the publication of the first works of Johnson and Schottky [1, 2]. A large number of original papers and reviews concerning $1/f^{\gamma}$ noise in solids (e.g., metal and resistive films) have been published during the last three or four decades [3 – 10]. This kind of noise is also referred to as excess noise, flicker noise (FN), or $1/f$ noise.

The latest publications on $1/f$ noise are reviewed in Ref. [11], the authors of which consider alternative models of $1/f$ noise and present data obtained by wavelet analysis of time series of noise signals.

At present, certain researchers believe flicker fluctuations in solids to be thermodynamically equilibrated even though thermodynamic equilibrium is known to be an abstract notion, there being no strictly equilibrated systems in nature. $1/f^{\gamma}$ fluctuations in homogeneous materials (metal and resistive layers, semiconductors, etc.) are associated with conduction (resistance) fluctuations that occur even in the absence of an electric current through the sample. The passing current only makes apparent fluctuations in the current-independent part of the sample's resistance. For this reason,

the term 'current noise', used in some publications [6] to denote equilibrium flicker noise, appears somewhat illogical.

The equilibrium nature of resistance fluctuations was confirmed by Voss and Clarke [10] by direct measurement of thermal noise fluctuations in InSb and island niobium films in the absence of current flowing through the sample. These fluctuations had a $1/f$ spectrum and were observed when a direct, sinusoidal, or pulse current passed through the sample. The spectrum of $1/f$ noise was the same regardless of the measurement methods. These data indicate that neither direct nor alternating current induced $1/f$ noise in the above experiments; rather, it was due to equilibrium fluctuations of the sample's resistance. We will call such fluctuations equilibrium flicker noise (EFN) or equilibrium $1/f$ noise. For this type of fluctuations, power spectral density (PSD) shows quadratic-in-current dependence, and the exponent γ is, as a rule, close to unity.

In conducting films, EFN coexists with noise having the spectrum of the form $1/f^{\gamma}$ that arises directly from the passage of current through the sample [3] or from other external impacts (radiation, deformation, etc.). In what follows, this type of noise will be referred to as nonequilibrium flicker noise (NEFN) or nonequilibrium $1/f^{\gamma}$ noise. Dependence of its PSD on the current can be considerably different from the quadratic, while the exponent γ deviates from unity and often takes the value of $\gamma \geqslant 2$.

In the general case, EFN and NEFN co-exist. Usually, measurements at a direct current yield total FN. Relative contributions of EFN and NEFN to the overall flicker-noise power differ depending on measuring conditions (current strength, temperature), microstructure, and other properties of the sample (grain size, presence of heterogeneous inclusions, mechanical stress, etc.).

Despite a large number of publications on $1/f$ noise in conducting films, there are still questions awaiting unequivocal answers. Sometimes, such questions arise from the fact that studies of $1/f$ noise usually measure total PSD of equilibrium and nonequilibrium flicker noise which makes it difficult to analyse the results obtained. At a low current density, NEFN is frequently masked by equilibrium flicker noise, although NEFN may prevail at a high current density. This probably explains why nonequilibrium $1/f^{\gamma}$ noise in conducting films is still so poorly known. At the same time, in many cases, only NEFN carries information about defects and damages in the crystal lattice of metals and semiconductors and serves as an informative characteristic of the quality of various materials and reliability of semiconductor devices and integrated microcircuits (IMCs). It is NEFN that is used to forecast electromigration (EM) stability of thin-film conductors [12–14].

Over the last few years, new properties of NEFN in conducting films and contacts have been reported, which calls for the analysis and systematization of the currently available data. This review is the first attempt to summarize and analyse theoretical and experimental information on NEFN in metal and alloy films, film resistors, and contacts for working out general concepts of the physical mechanisms underlying NEFN in these systems.

2. Concise information on equilibrium flicker noise (EFN)

Many experimental findings indicate that EFN in metal films stems from fluctuations of current carrier mobility. Mechanisms giving rise to equilibrium $1/f$ noise in metals vary. One consists of fluctuations in the mobility of carriers scattered by the lattice [15–17] or vacancies [18], another of generation-annihilation of quasi-equilibrium vacancies in the film sample [8]. Fluctuations in the number of quasi-equilibrium vacancies in a metal film in their turn lead to fluctuations of current carrier mobility.

2.1 EFN model related to fluctuations in the mobility of current carriers scattered by phonons

In 1969, Hooge and Hoppenbrouwers proposed to describe $1/f$ noise in metal films by an empirical formula for the relative PSD of voltage V (or resistance R) fluctuations [15], which has the form

$$S(f) = \frac{S_{\mathrm{V}}(f)}{V^2} = \frac{S_{\mathrm{R}}(f)}{R^2} = \frac{\alpha_{\mathrm{H}}}{N_0 f}\ \mathrm{Hz}^{-1}\,, \tag{2.1}$$

where α_{H} is the Hooge constant, $\alpha_{\mathrm{H}} = 2 \times 10^{-3}$, and N_0 is the number of charge carriers in the sample estimated from the carrier concentration n_{c} and effective sample volume V_{eff},

$$N_0 = n_{\mathrm{c}} V_{\mathrm{eff}}\,. \tag{2.2}$$

Structurally homogeneous metal films with a low concentration of stable and mobile defects have the $1/f$ noise level defined by the Hooge formula (2.1) at $\alpha_{\mathrm{H}} = 2 \times 10^{-3}$.

According to the generally accepted hypothesis, $1/f$ noise described by the Hooge formula (2.1) arises as a result of fluctuations in the mobility of charge carriers scattered by phonons. That $1/f$ noise is induced by fluctuations of a part of the lattice mobility μ_{b} is confirmed by experiments showing a decrease in the $1/f$ noise level in semiconductors with a decreasing contribution of carrier scattering by phonons to the overall resistance of the sample. Such a decrease was achieved in experiments by introducing additional stable impurities into the semiconducting sample [16]. The $1/f$ noise level observed in such samples was possible to calculate from formula (2.1) if constant α_{H} was substituted by the Hooge parameter α defined as [16, 17]

$$\alpha = \alpha_{\mathrm{H}} \left(\frac{\mu}{\mu_{\mathrm{b}}}\right)^2, \tag{2.3}$$

where μ is the resultant mobility taking into account carrier scattering by the lattice and the defects. Each scattering mechanism by itself determines current carrier mobility: a) lattice mobility μ_{b}; b) mobility μ_{def} associated with scattering by defects. If the two mechanisms act simultaneously, the following expression holds for the resultant mobility μ:

$$\frac{1}{\mu} = \frac{1}{\mu_{\mathrm{b}}} + \frac{1}{\mu_{\mathrm{def}}}\,. \tag{2.4}$$

This is the Mattissen rule. According to the major assumption of the mobility fluctuation model, only that part of mobility which is due to the scattering by the lattice (phonons) undergoes fluctuations. Hence,

$$\delta\mu = \left(\frac{\mu}{\mu_{\mathrm{b}}}\right)^2 \delta\mu_{\mathrm{b}}\,, \tag{2.4a}$$

giving rise to expression (2.3) for the parameter α [17]. In this case, the Hooge constant in (2.1) $\alpha_{\mathrm{H}} = \alpha_{\mathrm{b}} = 2 \times 10^{-3}$ is

related to the lattice scattering mechanism. For the PSD of fluctuations in lattice S_b and resultant S_μ mobilities, the following equation can be written [17]:

$$\frac{S_R}{R^2} = \frac{S_\mu}{\mu^2} = \frac{\alpha}{fN_0}\,, \qquad \frac{S_b}{\mu_b^2} = \frac{\alpha_H}{fN_0}\,. \tag{2.5}$$

The Hooge parameter α for many semiconducting materials and metals was experimentally found to lie in the range of $10^{-8} < \alpha < 10^{-1}$ [8, 16].

It is supposed that $1/f$ noise in lattice scattering originates from fluctuations in the scattering cross section of acoustic phonons. Experiments by Musha and co-workers on light scattering from acoustic phonons in quartz have shown that scattered light intensity fluctuates with a $1/f$-like spectrum [19]. It is supposed that the number of acoustic phonons per mode fluctuates near its mean value with the $1/f$ spectrum. However, there is still no model giving an analytical expression for the phonon noise with such a spectrum.

2.2 Vacancy model of EFN

The vacancy mechanism of equilibrium $1/f$ noise, the physical model of which was developed in [8], implies fluctuations of film conduction due to fluctuations in the number of quasi-equilibrium vacancies that require a relatively small energy to form and migrate. Generation of these fluctuations is unrelated to the passage of current through the sample.

Thin metal films have an inhomogeneous structure with a variety of vacancy sources (sinks) non-uniformly distributed throughout the bulk. In sinks, vacancies may be created or annihilated. The internal energy of vacancy formation varies from one source to another because an atom gives rise to vacancies by breaking a different number of bonds depending on its position (at the boundary of a grain, dislocation, or step, at the pore surface, etc.) [20].

The crystalline structure of a real metal film is not in thermodynamic equilibrium, and its free energy is enhanced by numerous defects present in the film. Being sources and sinks of vacancies, these defects change their position upon emitting or absorbing vacancies, i.e., dislocations can move and pores grow. The concentration of microdefects in the film is reduced by annealing. After annealing, at lower temperatures the defects may be fixed, i.e., they move very slowly or do not move at all. In such a situation, each source has its own quasi-equilibrium concentration of vacancies [20]. Neither emission nor absorption of vacancies by a source leads to a change in the film's free energy. In this sense, the film remains in a quasi-equilibrium (or locally equilibrium) state and the flicker noise stemming from vacancy number fluctuations may be regarded as quasi-stationary and quasi-equilibrium.

Upon a change of external conditions (temperature, current, mechanical stress, etc.), a film may undergo transition to a nonequilibrium state and give rise to nonequilibrium $1/f$ fluctuations. This type of non-equilibrium $1/f$ noise is considered in Section 7.

At thermodynamic equilibrium, the vacancy creation and annihilation rates are identical, and the average vacancy concentration remains constant in time. The vacancy lifetime τ_v in a film depends on the distance L_v between the sinks and is defined by the relation [20]

$$\tau_v = \frac{L_v^2}{\pi^2 D_v}\,, \tag{2.6}$$

where D_v is the vacancy diffusion coefficient.

A set of time constants τ_v is related to the activation energy distribution for vacancy diffusion coefficient D_v [20, 21] and to the distribution of distances L_v between vacancy sinks which are random variables in the film volume. The randomness of vacancy diffusion activation energy stems from a variety of structural imperfections. Owing to the nonuniform distribution of sinks over the bulk of real metal films, they have a large set of relaxation times associated with the vacancy creation and annihilation mechanism responsible for the $1/f$ noise over a wide frequency range, from a minimum frequency f_l to a maximum one f_h [8, 22].

It is assumed that generation of a $1/f$ noise takes place via the creation of vacancies due to the internal energy of the crystal following statistical laws. The process involves defects with a large set of activation energies which makes it possible to explain the $1/f$-like spectrum in a wide frequency range as a superposition of many random relaxation processes [23, 24]. Review [8] presents experimental data for a Mo film suggesting a broad range of activation energies under formation of the $1/f$ noise energy spectrum, from a minimum frequency $f_l \approx 4 \times 10^{-9}$ Hz to a maximum one $f_h \approx 10^{10}$ Hz. Also, the review offers a physical substantiation of the presence in metal films of a wide range of activation energies for the processes of creation-annihilation of quasi-equilibrium vacancies and the existence of a large set of relaxation times that accounts for $1/f$ noise in a broad frequency band. In Refs [8, 22], the known method for the summation of relaxation processes with different time constants [23, 24] was employed to analyse the vacancy mechanism of $1/f$ noise in metal films. An expression was obtained for the PSD of $1/f$ noise over a frequency range from f_l to f_h as a result of the superposition of many relaxation processes connected with the creation and annihilation of quasi-equilibrium vacancies:

$$S_{V_0} = \frac{KU_0^2\overline{\Delta n_{v0}^2}}{f} = \frac{KU_0^2 n_{v0}}{N_a f}\ \mathrm{V^2\,Hz^{-1}}\,, \tag{2.7}$$

where K is a constant for the film sample being tested and $n_{v0} = N_{v0}/N_a$ is the atomic concentration of quasi-equilibrium vacancies at temperature T. Here, N_{v0} and N_a are the numbers of quasi-equilibrium vacancies and atoms in the sample, respectively.

It is assumed in the derivation of formula (2.7) that the mean square of fluctuations in the number of quasi-equilibrium vacancies in the sample (fluctuation dispersion) is equal to their mean number N_{v0} [23, 24]:

$$\overline{(\Delta N_{v0})^2} = N_{v0}\,.$$

The dispersion of fluctuations in the atomic concentration of quasi-equilibrium vacancies is then

$$\overline{\Delta n_{v0}^2} = \frac{n_{v0}}{N_a}\,.$$

Because, according to Ohm's law, the voltage drop in a film sample is

$$U_0 = RI_0\,,$$

where R is the sample resistance and I_0 is direct current, expression (2.7) can be written as

$$S_{v0} = \frac{K_1 I_0^2\,\overline{\Delta n_{v0}^2}}{f}\ \mathrm{V^2\,Hz^{-1}}\,. \tag{2.7a}$$

Here, K_1 is a constant for the film sample being tested: $K_1 = KR^2$.

It is known that the atomic concentration of quasi-equilibrium vacancies n_{v0} in (2.7) and (2.7a) is defined as [21]

$$n_{v0} = A_v \exp\left[-\frac{E_v}{kT}\right], \tag{2.8}$$

where A_v is the entropy factor [21], which, for films, may be significantly greater than unity [8]; E_v is the activation energy of vacancy formation; k is the Boltzmann constant; and T is the absolute temperature.

The validity of the vacancy model of $1/f$ noise was confirmed in numerous experiments designed to evaluate the effects of various factors (film aging and annealing) on the $1/f$ noise level and the dependence of $1/f$ noise PSD on internal mechanical stress, temperature, film microstructure, etc. [8]. An important argument in favor of the vacancy mechanism of $1/f$ noise in metal films is the relationship between the $1/f$ noise level and the cubic nonlinearity of CVC found experimentally and confirmed by computation [25, 26]. The mechanism of electron scattering by quasi-equilibrium vacancies produces both cubic nonlinearity of CVC and equilibrium $1/f$ noise. These experimental results have been discussed at length in Ref. [8].

2.3 Temperature dependence of EFN

The component of EFN associated with scattering by phonons shows a weak temperature dependence [15]. In this case, the temperature dependence of $1/f$ noise PSD is largely determined by a weak temperature dependence of lattice mobility μ_b of the current carriers in (2.3).

At the same time, the dependence of the EFN PSD caused by the creation and annihilation of quasi-equilibrium vacancies [in agreement with (2.7a) and (2.8)] displays activation temperature dependence with the activation energy E_v typical for the process of vacancy formation at grain boundaries, micropores, and other defects of crystal lattice. Many experiments have demonstrated that the minimal activation energy E_v corresponds to the work necessary to break one or two bonds in the crystal lattice of a metal.

3. General information about nonequilibrium flicker noise (NEFN)

3.1. Current-voltage characteristic of a film sample

The resistance of any real two-terminal network can be represented in the form

$$R(I_0, t) = R_0(t) + N(I_0, t), \tag{3.1}$$

where $R_0(t)$ and $N(I_0, t)$ are components of the total resistance not dependent on direct current I_0 and dependent on it, respectively. Time t dependence reflects the fluctuation process.

The current-dependent part of resistance of a two-terminal network $N(I_0, t)$ can be approximated in different ways. When the current $I_0 = 0$, the term $N(I_0, t) = 0$. If the resistance $R(I_0, t)$ is approximated as a power series [27, 28] with the number of terms $k + 1$, then

$$R(I_0, t) = R_0(t) + \sum_{n=1}^{k} R_n(t)\, I_0^n, \tag{3.2}$$

where R_n are coefficients to the nth power of the current ($n = 0, 1, 2, \ldots, k$).

The second item in (3.2) is the part of resistance R depending on the current I_0. Different terms of (3.2) are due to different mechanisms of transfer and scattering of current carriers. Such mechanisms may be scattering by phonons and mobile defects (vacancies), which contributes to the cubic nonlinearity of the current-voltage characteristic (CVC) [8], and overbarrier and tunnel emission in discontinuous films [29, 30].

Because higher-than-zero coefficients in series (3.2) ($n = 1, 2, 3, \ldots$) contribute to the resistance of a two-terminal network (hence, to its fluctuations) only at current $I_0 > 0$, fluctuations of these coefficients may be regarded as related to nonequilibrium fluctuations of film conduction caused by the passage of current through the sample. Fluctuations of coefficient $R_0(t)$ give equilibrium $1/f$ noise.

In case of approximation by a power function, resistance of the conducting sample is represented in the form [31]

$$R(I_0, t) = R_0(t)\left[1 + Z(t)\, I_0^{\beta-1}\right], \tag{3.3}$$

where $Z(t)$ is the CVC nonlinearity parameter and β is the exponent specifying the shape of CVC nonlinearity.

In certain cases (e.g., for commercial quality control of electronic devices and IMC), approximation by power function (3.3) may be preferable to approximation by power series (3.2) [31].

At the same time, the CVC of a resistance R contains both linear (i.e., Ohm's law) and nonlinear parts, regardless whether R is approximated by (3.2) or (3.3), and can be described by the expression

$$V(I, t) = R(I, t)\, I = R_0(t)\, I + N(I, t)\, I, \tag{3.4}$$

where V is the voltage drop and I is the current through the sample containing, in the general case, both direct and alternating components.

The first term in (3.4) gives Ohm's law while the term $N(I, t)\, I$ defines the CVC nonlinearity level depending on all nonlinear terms, in agreement with the chosen approximation (3.2) or (3.3), and expressed in Ohms. The level of CVC nonlinearity can also be expressed in relative units:

$$K_N = \frac{N(I)}{R_0}, \tag{3.4a}$$

where K_N is the dimensionless CVC nonlinearity coefficient and $N(I)$ and R_0 are CVC coefficients averaged over time. The condition of low CVC nonlinearity may be represented in the form [31]

$$N(I) \ll R_0 \tag{3.5}$$

or, for the dimensionless nonlinearity coefficient K_N (3.4a), in the form

$$K_N = \frac{N(I)}{R_0} \ll 1. \tag{3.5a}$$

It is worth mentioning that CVC nonlinearity coefficients introduced earlier by Kirbi [32] and in Ref. [8] are defined by the ratio of the amplitude U_3 or U_2 of the third or second harmonic, respectively, to the amplitude U_1 of the funda-

mental frequency signal (in the case of harmonic influence on the sample) and characterize cubic (or quadratic) CVC nonlinearity. Unlike those coefficients, nonlinear coefficients $N(I)$ and $K_N = N(I)/R_0$ introduced by relations (3.4) and (3.4a) in the present paper describe the total CVC nonlinearity level resulting from the contribution of all its nonlinear terms.

3.2 Dependence of nonequilibrium flicker noise PSD on the current

In the absence of a correlation between current-dependent and current-independent parts of resistance R in (3.1), spectral density (SD) of voltage V flicker fluctuations on a two-terminal network $S_V(f)$ at a given direct current I_0 through it is defined, in the general case, by the expression

$$S_V(I_0, f) = S_{RL}(f) I_0^2 + S_{RN}(I_0, f) I_0^2 , \tag{3.6}$$

where $S_{RL}(f)$ and $S_{RN}(I_0, f)$ are SDs of fluctuations of the current-dependent and independent parts of resistance R, respectively.

The first and second terms in expression (3.6) for spectral density of voltage V fluctuations on a two-terminal network are determined by equilibrium (linear) and nonequilibrium (nonlinear) fluctuations of resistance, respectively.

In measuring $1/f$ noise PSD of a two-terminal network at a given current I_0, both components of PSD in (3.6) are measured simultaneously, which precludes the assessment of individual contribution of each CVC component to the $1/f$ noise level and the separation of NEFN from the total flicker-noise power $S_V(I_0, f)$. At a small current I_0, the nonequilibrium $1/f$ noise is in many cases masked by the equilibrium one (for high-quality metal films, this usually occurs at current density $j_0 \leqslant 10^6$ A cm^{-2}).

For an element with weak nonlinearity, such as a metal film, the terms of the power series in (3.2) rapidly decrease with number n, and expression

$$\overline{R_0} \gg \overline{R_n} \quad (n = 1, 2, 3, \ldots)$$

is correct for typical working currents (here, $\overline{R_0}$ and $\overline{R_n}$ are coefficients $R_0(t)$ and $R_n(t)$ averaged over time). In cases of great practical importance, this condition permits us to keep only three terms in expansion (3.2). Then, expression

$$V(t) = R_0(t) I_0 + R_1(t) I_0^2 + R_2(t) I_0^3 \tag{3.7}$$

holds for CVC. In this case, voltage V fluctuations on a film sample through which direct current I_0 flows are defined in the following way:

$$\Delta V(t) = \Delta R_0(t) I_0 + \Delta R_1(t) I_0^2 + \Delta R_2(t) I_0^3 , \tag{3.8}$$

where $\Delta V(t) = V(t) - \overline{V}$ ($\overline{V}$ is the time-averaged voltage drop on a film sample) and $\Delta R_n(t) = R_n(t) - \overline{R_n}$ $(n = 0, 1, 2)$.

In the absence of a correlation between coefficients $R_0(t)$, $R_1(t)$, and $R_2(t)$ in (3.7), noise PSD at a given direct current I_0 is expressed as

$$S_V(I_0, f) = S_{R_0}(f) I_0^2 + S_{R_1}(f) I_0^4 + S_{R_2}(f) I_0^6 , \tag{3.9}$$

where S_{R_0}, S_{R_1}, and S_{R_2} are SDs of fluctuations of coefficients R_0, R_1, and R_2 in expansion (3.2) and expression (3.7) for CVC.

When there is a correlation between fluctuations of coefficients $R_n(t)$, the dependence $S_V(I_0, f)$ additionally contains terms with the third and fifth powers of the current. For example, correlation between coefficients $\Delta R_0(t)$ and $\Delta R_1(t)$ in (3.7) leads to the appearance in expression (3.9) for noise PSD of a term showing cubic current dependence in the form

$$S_V(I_0) \propto \overline{\Delta R_0(t)\, \Delta R_1(t)}\, I_0^3$$

(the bar indicates averaging over time). The cubic dependence of noise PSD on the current in Al films was observed by Neri [14] for electromigration noise.

Thus, nonequilibrium conduction fluctuations result in the deviation of the current dependence of $1/f$ noise PSD on the quadratic one, which is especially noticeable at high currents. Only EFN defined by the first term in expression (3.9) is observed at small currents.

4. Methods of experimental studies of nonequilibrium flicker fluctuations in conducting films and contacts

Two known measuring techniques can be used to separate NEFN from the total FN power. Both are based on the excitation of a test film sample by signals of different form [27, 31, 33, 34]. The two methods are analysed below.

4.1 Voltage spectrum of the signal-response in a film sample under harmonic test influence

Given a flow of sinusoidal current $I_1 \sin(\omega_1 t)$ with amplitude I_1 and frequency f_1 (angular frequency $\omega_1 = 2\pi f_1$) through a nonlinear film sample, voltage $U(t)$ spectrum shows signal-response harmonics. For the voltage $U(t) = R(I_1, t) I_1 \sin(\omega_1 t)$, taking into account (3.2), it is possible to write [27]

$$U(t) = U_0(t) + \sum_{n=1}^{k} U_n(t) \sin(n\omega_1 t) , \tag{4.1}$$

where $U_0(t)$ is the voltage of the constant component (zeroth harmonic), $U_n(t)$ is the voltage amplitude of the nth harmonic, and $U_0(t)$ and $U_n(t)$ are random functions of time due to fluctuations of coefficients $R_n(t)$ in (3.2).

For a weakly nonlinear sample, such as a metal film or film contacts, it is sufficient to consider three first terms in expansion (4.1). In this case, amplitudes of harmonics — zeroth (constant constituent) U_0, second U_2, and third U_3 — are defined through coefficients of series (3.2) by the following expressions [27]:

$$U_0(t) = 0.5 R_1(t) I_1^2 , \tag{4.2}$$

$$U_2(t) = 0.5 R_1(t) I_1^2 , \tag{4.3}$$

$$U_3(t) = 0.25 R_2(t) I_1^3 . \tag{4.4}$$

For the fundamental frequency voltage, the following relation holds:

$$U_1(t) = R_0(t) I_1 + 0.75 R_2(t) I_1^3 \approx R_0(t) I_1 . \tag{4.5}$$

The term with coefficient R_2 makes an insignificant contribution to amplitude U_1. The so-called $1/\Delta f$ noise of the sample as a random modulation of the sinusoidal test

signal studied in Refs [35–38] arises from fluctuations of the linear part of resistance $R_0(t)$ and is associated with equilibrium conduction fluctuations. At the same time, fluctuations of coefficients R_1 and R_2 (quadratic and cubic terms of CVC) lead to noise-induced modulation of the zeroth, second, and third harmonics of the signal-response and produce NEFN. It follows from Eqns (4.2)–(4.4) that the zeroth and second harmonics are due to quadratic nonlinearity of CVC and proportional to I_1^2 while the third harmonic is due to cubic nonlinearity of CVC and proportional to I_1^3.

4.2 Method for measuring amplitude fluctuation spectra of signal-response harmonics in a sample under harmonic test influence

Methods of experimental studies of sinusoidal signal amplitude fluctuations are described at length in monograph [39]. Investigations into NEFN usually include measurements of spectral density of amplitude fluctuations of the third, $U_3(t)$, second, $U_2(t)$, or zeroth (constant component) $U_0(t)$ harmonics [27, 33].

The harmonic amplitude fluctuation spectrum is measured after detection of the second or the third harmonic signals. It is worth noting that prior to the detection, the signal spectrum for each harmonic is discrete with a symmetric base near the line due to fluctuations of its amplitude [39]. After the detection of a signal undergoing amplitude fluctuations (random amplitude modulation), $1/f^{\gamma}$ noise has a continuous spectrum concentrated near the zero frequency [39].

Here is a brief description of a device for measuring energy spectra of sinusoidal signal amplitude fluctuations [39] and amplitude fluctuation spectra of signal-response harmonics that was used to study NEFN in molybdenum films [27, 33].

The measuring device consists of the following units.

(1) Generator of sinusoidal signals with a very small harmonic content (below — 150 dB) from which the first harmonic voltage (fundamental frequency) is transmitted onto the film sample being tested. Higher harmonics in the test signal are usually suppressed with the help of a low-pass filter placed between the standard generator and the test sample. In Refs [27, 33], the test signal frequency is chosen to be $f_1 = 10$ kHz.

(2) Selective amplifier designed to separate the signal of fundamental frequency f_1 for studying $1/\Delta f$ noise [35–38].

(3) Highly sensitive selective amplifiers to separate and amplify the signal-response of the second ($2f_1$) and the third ($3f_1$) harmonics in NEFN studies (or an amplifier of constant component voltage in the study of the zeroth harmonic fluctuations) [33] arising from the CVC nonlinearity of the sample. In order to suppress the first harmonic in the signal-response spectrum of the sample, high-pass filters are inserted at the inputs of the amplifiers for the second and the third harmonics.

(4) Amplitude detector to register signals of fundamental frequency f_1 and signal-responses of the second and third harmonics. The latter are modulated in amplitude by nonequilibrium flicker noise.

(5) Low-pass filters (LPFs) placed after the detector effectively suppressing signals with frequencies f_1, $2f_1$, and $3f_1$, i.e., letting through only low (compared with f_1, $2f_1$, and $3f_1$) frequencies. Due to this, there are no output oscillating signals from the LPFs.

(6) Highly sensitive low-frequency amplifier placed after the LPF from which the NEFN being tested is fed into a spectrum analyzer or processed by a computer.

The results of measurements of amplitude fluctuation SD for the zeroth, second, and third harmonics $S_{\mathrm{U}_n}(f)$ ($n = 0, 2, 3$) may be used to derive the SD of coefficients $R_1(t)$, $R_2(t)$, and $R_3(t)$ fluctuations in expansion (3.2) for film resistance in accordance with (4.2)–(4.4). The SD of harmonic amplitude fluctuations being known, it is possible to calculate the SD of the magnitude of noise amplitude modulation of signal-response harmonics $m_0(f)$, $m_2(f)$, and $m_3(f)$ using the formula [39]

$$m_n(f) = \frac{S_{\mathrm{U}_n}(f)}{U_n^2 K_{\mathrm{det}}^2} = \frac{S_{\mathrm{R}_n}(f)}{R_n^2} \quad (n = 0, 2, 3)\,, \tag{4.6}$$

where U_n is the amplitude of the nth harmonic and K_{det} is the transfer coefficient of the detector.

Spectral densities of fluctuations $S_{\mathrm{R}_n}(f)$ for coefficients $R_n(t)$ can be computed using expressions (4.2)–(4.4).

4.3 Method for measuring voltage fluctuations of the constant component of the sample's signal-response under pulse test influence

This method consists of exciting a test sample with nonlinear CVC by a train of rectangular pulses of a current having a constant amplitude and zero mean value. The detection of the pulses results in constant component voltage (CCV) U_{C} on the sample.

The structural scheme of a simplest measuring device for determining the CCV and the spectral density of its fluctuations is presented in Fig. 1 [31]. Sample R is excited by a test signal in the form of focused current pulses (bipolar current pulses) generated on the sample when pulses from the generator (*1*) are transmitted through a separating capacitor with capacity C. Constant component voltage U_{C} arising from the detection of current pulses on sample R with nonlinear CVC is separated by the low-pass filter (*2*) and measured by the voltmeter (*3*); its amplitude fluctuations are measured by the spectrum analyzer (*4*) and processed by a computer [31, 40]. (Note that the voltage $U_{\mathrm{C}} = 0$ when the resistance R is constant and independent of the current.) In this way, NEFN of sample R (see Fig. 1) is separated from the total $1/f$ noise power.

It appears appropriate to represent here some relations derived in [31, 40] to substantiate the method for measuring nonlinear CVC parameters and nonequilibrium flicker noise under the pulse test influence.

In order to avoid overheating the sample by Joule heating at large pulse currents, the pulse duty cycle Q is chosen from the condition

$$Q = \frac{T}{t_{\mathrm{p}}} \geqslant 2\,, \tag{4.7}$$

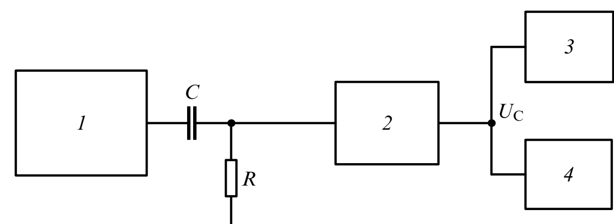

Figure 1. Diagram of a setup for measuring the constant component voltage U_{C} and the spectral density of its fluctuations [31]: R is the sample being tested, *1* is the generator of current pulses, *2* is a low-pass filter, *3* is a voltmeter, *4* is a spectrum analyzer

where T is the pulse period and t_p is the length of current pulses.

A noninertial approximation is considered, the condition of which implies the absence of the CCV U_C dependence on the pulse period with an amplitude I_p.

Calculations made in [31, 40] indicate that, under constraints (3.5) and (4.7), the CVC nonlinearity level in expression (3.4) is proportional to the constant voltage component $U_C(I_p, t)$, so that

$$N(I,t)I \cong \frac{Q^3}{(Q-2)(Q-1)}\,U_C(I_p,t)\,. \tag{4.8}$$

At $Q = 12$, as recommended in [31, 40] for practical applications, expression (4.8) gives for the nonlinear part of CVC in (3.4)

$$N(I,t)\,I \cong 12U_C(I_p,t)\,. \tag{4.8a}$$

In this case, the PSD of nonlinear flicker noise $S_{VN}(f)$ is related to the SD of CCV fluctuations $S_C(f)$ by expression

$$S_{VN}(f) \cong \left[\frac{Q^3}{(Q-2)(Q-1)}\right]^2 S_C(f)\,. \tag{4.9}$$

Based on (4.8) and (4.9), it is possible to determine the CVC nonlinearity level and compute the nonequilibrium component of flicker-noise PSD.

5. Results of investigations into nonequilibrium flicker noise in conducting films

In what follows, we analyse results of published experimental studies on NEFN in metal and alloy films with different physical mechanisms for its generation. The analysis indicates that for certain types of NEFN, $\gamma \geqslant 2$, although for other NEFN the exponent γ is close to unity.

5.1 Nonequilibrium flicker noise in metal and alloy films due to the generation of excess vacancies

At sufficiently high current densities across metal and alloy film samples, the current dependence of noise PSD deviates from the quadratic law even if the change of film resistance caused by Joule heating is excluded. This can be accounted for by the appearance of NEFN associated with film resistance fluctuations due to fluctuations in the number of excess vacancies generated by its current heating. This NEFN is a stationary or quasi-stationary noise.

5.1.1 Theoretical analysis. The contribution of vacancies to film resistivity ρ_v is defined as [41]

$$\rho_v = A_1 n_v(t) = \frac{A_1 N_v(t)}{N_a}\,, \tag{5.1}$$

where A_1 is a constant depending on the metal (for aluminium, $A_1 = 220$ μΩ cm, see [41]).

When the equilibrium $1/f$ noise has a vacancy nature, expression (2.7a) holds for noise PSD. As the current through the sample grows, the film temperature increases; this leads to a rise in the number of vacancies in accordance with (2.8). It may be supposed that nonequilibrium noise will prevail over equilibrium noise when the number of vacancies additionally generated due to film overheating exceeds their equilibrium number observed at room temperature. Refs [28, 42] report estimates of the current at which concentrations of excess vacancies produced in a metal film by Joule heating become equal to their equilibrium concentrations. These results are presented below.

A rise in film temperature T by ΔT relative to room temperature T_0 is defined through time-averaged electrical resistance $\overline{R}$ of the sample averaged over time and thermal resistance R_T by the relation [43]

$$\Delta T = T - T_0 = R_T \overline{R} I_0^2\,. \tag{5.2}$$

The vacancy concentration in the sample is then

$$n_v = A_v \exp\left[-\frac{E_v}{k(T_0+\Delta T)}\right]. \tag{5.3}$$

At $\Delta T \ll T_0$, (5.3) gives

$$n_v \approx n_{v0} \exp\left(\frac{E_v \Delta T}{kT_0^2}\right), \tag{5.4}$$

where n_{v0} is the quasi-equilibrium vacancy concentration at room temperature:

$$n_{v0} = A_v \exp\left[-\frac{E_v}{kT_0}\right]. \tag{5.5}$$

After the expansion of the exponent in expression (5.4) in the Taylor series, and taking into account that $E_v \Delta T/(kT_0^2) \ll 1$ and substituting into it ΔT from expression (5.2), it is easy to obtain an expression for vacancy concentration in the film under current heating [28]

$$n_v \approx n_{v0}\left(1 + 2BI_0^2 + \frac{B^2 I_0^4}{2} + \ldots\right), \tag{5.6}$$

where $B = E_v \overline{R} R_T/(kT_0^2)$ is a constant coefficient.

In [28], an expression for the dispersion of fluctuations of atomic vacancy concentration during current heating of a film sample was obtained on the assumption that the mean-square of fluctuations of the vacancy number (fluctuation dispersion) $\overline{(\Delta N_v)^2} = N_v$, i.e., equals their mean number N_v [21], taking into consideration that, in this case, the dispersion of atomic concentration fluctuations of quasi-equilibrium vacancies $\overline{\Delta n_{v0}^2} = n_{v0}/N_a$. Using only the first three terms of expansion (5.6), it is found that

$$\overline{\Delta n_v^2} \approx \left(\frac{n_{v0}}{N_a}\right)\left(1 + 2BI_0^2 + 2B^2 I_0^4\right). \tag{5.7}$$

Expressions (2.7a) and (5.7) define $1/f$ noise PSD $S_V(f)$ at a given current I_0 so that

$$S_V = KI_0^2\left(\frac{n_{v0}}{N_a}\right)\frac{1 + 2BI_0^2 + 2B^2 I_0^4}{f}\,. \tag{5.8}$$

The first term in (5.8) $K_1 I_0^2 (n_{v0}/N_a)$ is related to fluctuations in the number of equilibrium vacancies in the sample and gives the usual quadratic current dependence of noise PSD characteristic of equilibrium flicker noise. Other terms in (5.8) define NEFN. The second one gives the dependence $S_V \sim I_0^4$. At current $I_0 = (2B)^{-0.5}$, the concentration of additionally generated vacancies in the film due to Joule

heating becomes roughly equal to their equilibrium concentration. At current $I_0 > (2B)^{-0.5}$, the second term in (5.8) is larger than the first one and NEFN exceeds EFN.

5.1.2 Some experimental results. Figure 2 shows dependences of $1/f$ noise PSD on direct current for a chromium film of thickness $h = 160$ nm and width $b = 0.37$ mm, having an enhanced concentration of vacancies [28]. The vacancy mechanism of $1/f$ noise in such films was confirmed by the activation dependence of noise PSD on temperature with an activation energy $E_v = 0.6$ eV (at a frequency of 35 Hz). The level of the observed $1/f$ noise was four-five orders of magnitude higher than that given by expression (2.1) (the concentration of carriers for the computation in [28] was taken to be $n_c = 1.7 \times 10^{22}$ cm^{-3}).

The dependences presented in Fig. 2 obey the $S_V \sim I^n$ law with a variable exponent n. As shown by the analysis, exponent n at current density $j < 3 \times 10^3$ A cm^{-2} is close to $n \approx 2.0$ and at $j > 10^4$ A cm^{-2} is as large as $n \approx 4.0$. At small currents, EFN appears due to fluctuations in the number of quasi-equilibrium vacancies in the sample. As the current grows, film temperature rises, which leads to an increase in the number of vacancies in conformity with expression (5.4). When the number of additionally generated vacancies exceeds their equilibrium number (corresponding to room temperature) due to film overheating, NEFN prevails over EFN.

In Ref. [28], the current $I_m = (2B)^{-0.5}$ is estimated at which the concentration of additionally generated excess vacancies in chromium films is equal to an equilibrium one. At the adopted numerical values for the sample being tested, $E_v = 0.6$ eV, $RR_T = 4 \times 10^5$ Ω K W^{-1}, $T = 300$ K, current $I_m = 4$ mA, and $j_m = 7 \times 10^3$ A cm^{-2}, in agreement with the current strength at which the slope of experimental curves in Fig. 2 changes.

Current dependences of $1/f$ noise similar to those for chromium films in Fig. 2 were found for thin-layer films of Ni/Cr alloy with resistance 500 – 4000 Ω [13] and for Al/Cu films (20% Cu by weight) deposited upon oxidized silicon substrates by thermal evaporation in a vacuum (film sample length $l = 1.3$ mm, width $b = 20$ μm, thickness $h = 300$ nm) [44]. In the latter work, the current dependence of $1/f$ noise PSD was close to quadratic at the current density $j_0 \leqslant 2.1 \times 10^6$ A cm^{-2} and roughly obeyed the $\propto j_0^4$ law at density $j_0 = (2.1 - 3.2) \times 10^6$ A cm^{-2}. Exponent γ specifying the shape of the spectrum varied in the range $\gamma = 1.07 - 1.22(\pm 0.05)$.

Figure 3 illustrates the current dependence of $1/f$ noise PSD for Ni/Cr films [13]. $1/f$ noise PSD shows power dependence on the current, such that $S_V \propto I_0^n$, with exponent $n \approx 2$ at $I_0 < 1.75$ mA and $n = 3.5 - 4.5$ at higher currents. Exponent γ for these films at $T = 300$ K in the range of current $I_0 = 0.5 - 3$ mA equals 1.3 and remains constant.

For Ni/Cr films at higher currents, Ref. [13] reports activation dependences of $1/f$ noise PSD on temperature represented by straight lines in the Arrhenius coordinates (Fig. 4). This finding confirms the activation mechanism of $1/f$ noise in the tested films. Activation energies observed in the experiment are $E_a = 0.34$ eV for current $I_0 = 3$ mA and $E_a = 0.31$ eV for current $I_0 = 2$ mA.

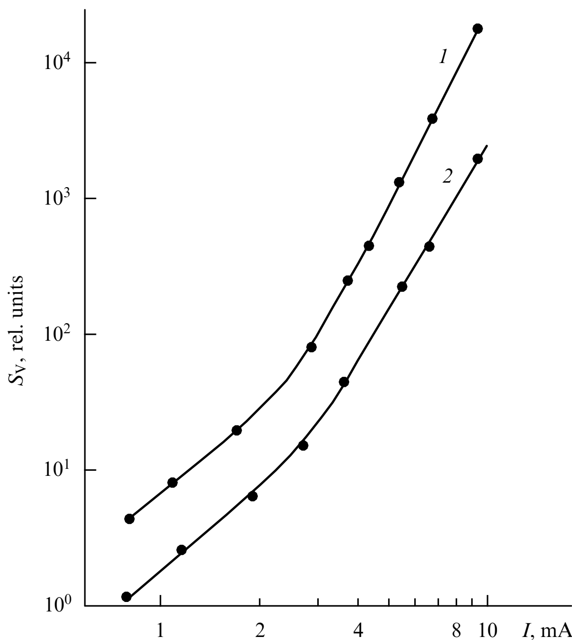

Figure 2. Current dependences of $1/f$ noise PSD for a chromium film 160 nm thick and 0.37 mm wide [28]: curve *1* — $f = 2$ Hz; curve *2* — $f = 5$ Hz.

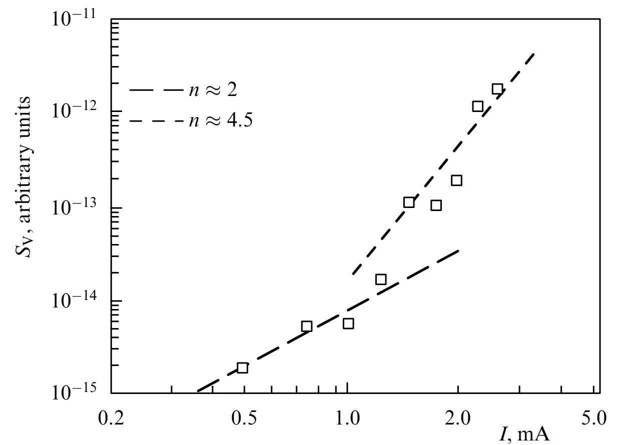

Figure 3. $1/f$ noise PSD of a Ni/Cr film vs. direct current; film resistance $R = 500$ Ω, $T = 300$ K [13].

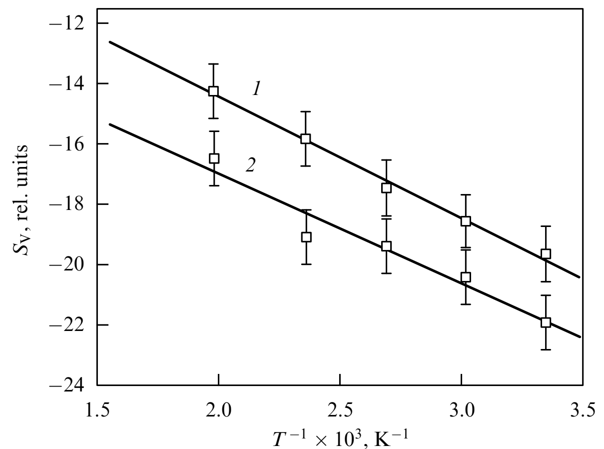

Figure 4. Temperature dependences of $1/f$ noise PSD for Ni/Cr films at different currents in the Arrhenius coordinates [13]: line *1* — $I_0 = 3$ mA; line *2* — $I_0 = 2$ mA.

The above data on $1/f$ noise in Cr, Ni/Cr, and Al/Cu films give evidence of the manifestation of the NEFN vacancy mechanism at a high current density attributable to the generation of excess vacancies by Joule heating of the sample. The PSD of NEFN shows activation temperature dependence whereas current dependence of noise PSD in the form of $S_V \propto j_0^4$ is related to the contribution of the term $2BI_0^2$ in expression (5.8) at high currents. Exponent γ for this type of NEFN is close to unity: $\gamma \approx 1-1.3$ [13, 28, 44].

5.1.3 NEFN induced by local heating of the film. Metal films with an inhomogeneous crystalline structure or nonuniform distribution of defects and admixtures accounting for their nonuniform surface resistivity undergo nonequilibrium conduction fluctuations under the effect of local overheating due to the appearance of high current density areas. Heating such areas above a certain temperature results in the intense generation of mobile lattice defects (largely vacancies) responsible for the production of NEFN at high current densities ($j_0 > 10^6$ A cm^{-2}) and for the current dependence of noise PSD in the form $S_V \propto I_0^4$, in accordance with expression (5.8).

Such an NEFN mechanism was observed in metal films experiencing electromigration (EM) damage [28]. Figure 5 shows dependences of relative SD of resistance fluctuations in an Al/Cr film on the squared direct current density: curve *1* — for an EM-damaged film sample, curve *2* — for a freshly manufactured undamaged sample. It follows from Fig. 5 that the relative SD of resistance fluctuations for the intact sample remained practically unaltered with increasing currents $j_0 < 2$ MA cm^{-2}. It means that $1/f$ noise PSD was $S_V \propto I_0^2$. Undamaged films were characterized by a low $1/f$ noise level with the Hooge parameter $\alpha = 8 \times 10^{-3}$ computed by using expression (2.5) based on the adopted carrier concentration $n_c = 1.8 \times 10^{23}$ cm^{-3} [28]. In intact films of Al/Cu alloy at the current density $j_0 < 2.2 \times 10^6$ A cm^{-2}, NEFN could be observed neither at room ($T = 297$ K) nor at a much higher ($T = 523$ K) temperature [28]. At the same time, the relative SD of resistance fluctuations for a damaged sample at currents $j_0 > 1$ MA cm^{-2} varied with the current as I_0^2 (curve *1* in Fig. 5). Hence, noise PSD was $S_V \propto I_0^4$. In other words, the EM-damaged film gave rise to NEFN as a result of the generation of excess vacancies induced by local overheating.

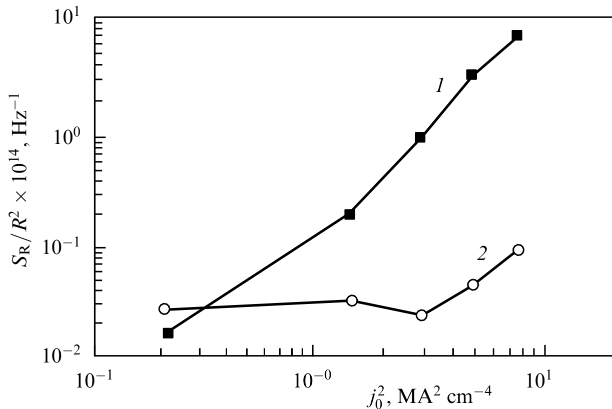

Figure 5. Plot of relative SD of resistance fluctuations in an Al/Cr film vs. squared direct current density [28]: curve *1* — for an EM-damaged sample; curve *2* — for an intact sample.

Metal films with a high concentration of stable defects and a low level of mobile ones at a small current density exhibit $1/f$ noise, the magnitude of which is significantly lower than predicted by the Hooge formula (2.1). This can be attributed to a decrease of parameter α in (2.3) related to the lowered resultant mobility μ in (2.4) due to the presence of stable defects. Such $1/f$ noise was observed in chromium films [45]. In these experiments, films were deposited upon oxidized silicon substrates by the thermal evaporation technique in an atmosphere of nitrogen. Due to the high nitrogen impurity level, film resistivity ρ_f was significantly higher than that of bulk chromium ρ_0, so that $\rho_f \approx 10\rho_0$.

Figure 6 shows the dependence of $1/f$ noise PSD for such films on the direct current density squared (curve *1*) and the results of calculations by the Hooge formula (2.1) on the assumption that $\alpha_H = 10^{-3}$ (curve *2*). The $1/f$ noise at the current density $j_0 \leqslant 5 \times 10^5$ A cm^{-2} does not exceed thermal noise and is about two orders of magnitude lower than defined by formula (2.1), in agreement with (2.3) at an almost 10-fold decrease of the resulting mobility μ in (2.4) caused by additional scattering of electrons from stable defects.

However, as current density grows up to $j_0 > 5 \times 10^5$ A cm^{-2}, the $1/f$ noise level begins to increase (Fig. 6, curve *1*) due to the development of nonequilibrium conduction fluctuations under the effect of local film overheating caused by the nonuniform distribution of stable defects. This leads to a deviation of the current dependence of $1/f$ noise PSD from quadratic at $j_0 \geqslant 1$ MA cm^{-2} and to a current-dependent change of $1/f$ noise PSD according to a power law so that $S_V \propto j_0^n$, where the exponent n increases with the current up to $n = 4$ and continues to grow thereafter (Fig. 6, curve *1*).

The appearance of NEFN due to local film overheating was confirmed in an experiment [45] designed to examine the effects of temperature on $1/f$ noise PSD in Cr films heated in a

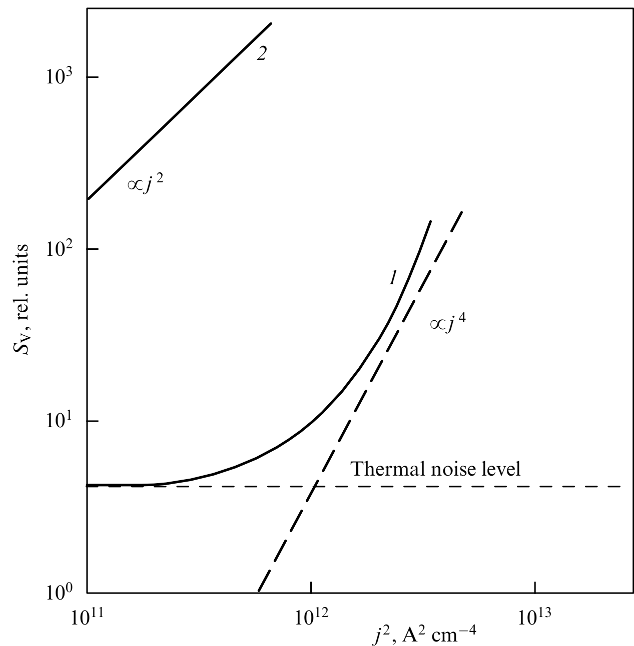

Figure 6. $1/f^2$ noise of a Cr film deposited in an atmosphere of nitrogen vs. direct current density squared (curve *1*) and the results of a computation using the Hooge formula (2.1) on the assumption that $\alpha_H = 10^{-3}$ (curve *2*) [45].

thermostat or subjected to current heating (in the latter case, the sample temperature was obtained from the calibration curve in which resistance was plotted against temperature). The temperature dependence of $1/f$ noise PSD for a film heated in the thermostat proved to be identical to that of a current-heated film. However, current heating resulted in a shift of the current dependence of $1/f$ noise PSD to the left by approximately 50 K suggesting that the noise started to increase at a lower temperature. This finding confirms that Cr films contain domains of nonuniformly distributed stable defects responsible for nonuniform conductivity, hence for nonuniform current density that underlies local film overheating and the resulting nonequilibrium flicker noise.

5.2 Electromigration $1/f^2$ noise

This type of NEFN is reported to occur in films of Al and its alloys at elevated temperatures and high current loads [12–14, 46–57]. As the current load increases, exponent γ reaches the value of 1–2 and even higher. For example, exponent γ for Al and Al/Si films was found to be $\gamma = 2-2.6$ at the current density $j_0 = (1.3-2.5)\times 10^6$ A cm^{-2} and temperature $T = 320-410$ K [54]. A component of NEFN with a $1/f^2$ noise spectrum is frequently referred to as electromigration (EM) $1/f^2$ noise.

EM $1/f^2$ noise at a direct current can be discovered by measuring noise PSD at frequencies below 1 Hz (usually in the range from 10 mHz to 1 Hz) because at higher frequencies it is masked by equilibrium $1/f$ noise for which $\gamma \approx 1$. In films of Al and its alloys, an NEFN component arises as a result of atomic migration along grain boundaries or across the crystal lattice [12–14].

Each component of equilibrium $1/f$ noise and nonequilibrium EM noise is produced by a different physical mechanism. The equilibrium $1/f$ noise in metal films (both annealed and unaffected by external impacts, e.g., deformation) results from fluctuations in the mobility of charge carriers scattered by the lattice or by quasi-equilibrium vacancies. This NEFN component is stationary $1/f$ noise. At the same time, EM $1/f^2$ noise is due to electrical mass transfer of the metal film material toward different sinks in the bulk (lattice diffusion) or along grain boundaries (GB diffusion). These processes give rise to irreversible changes in the film [58, 59]. This NEFN has a nonstationary nature.

At the same time, measurements of $1/f$ noise PSD at sinusoidal current ($1/\Delta f$ noise) [60] in alloy films of Al/Si(1%)/Cu(0.5%) sized $2 \times 100 \times 0.8$ μm^3 invariably yielded γ values in the range from 0.85 to 1.15. This can be accounted for by the absence of electromigration of metal atoms in the sinusoidal electric field [58].

5.2.1 Temperature dependence.

At a given current density j_0, electromigration $1/f^2$ noise PSD increases with temperature. Figure 7 depicts results of a study on $S_V(f)$ dependence of EM $1/f^2$ noise PSD at different temperatures for alloy films of Al/Si(1%) [14]. Curve BN representing the background noise of the measuring system was obtained by the substitution of a noiseless resistor for the film sample [12]. Figure 7 shows that the spectrum shape exponent γ increases with increasing temperature. Figure 8 illustrates the temperature dependence of EM $1/f^2$ noise PSD [14] for two frequencies $f_0 = 50$ mHz and $f_0 = 1$ Hz. Also shown are γ values for a frequency of 1 Hz deduced from the slope of dependences $S_V(f)$ plotted in logarithmic coordinates for the frequency range 0.5–1 Hz and γ values for a frequency of 50 mHz

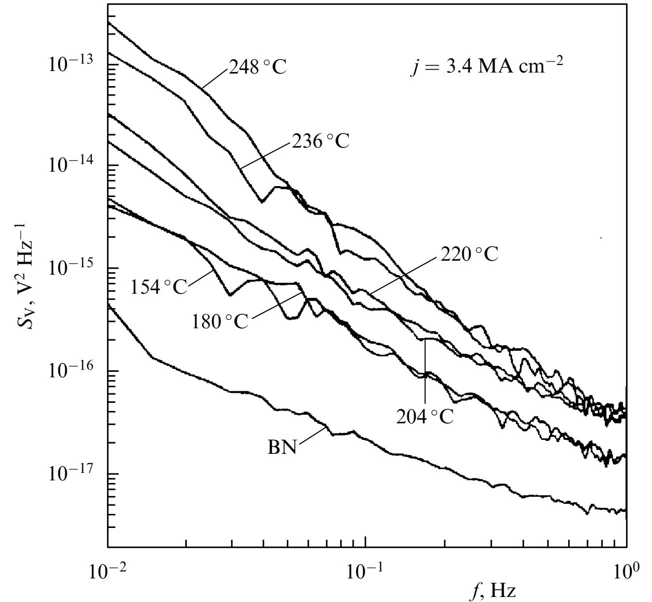

Figure 7. Dependences of $1/f^2$ noise PSD at direct current $j = 3.4$ MA cm^{-2} and different temperatures for an Al/Si(1%) film. Curve BN represents background noise of the measuring system [14].

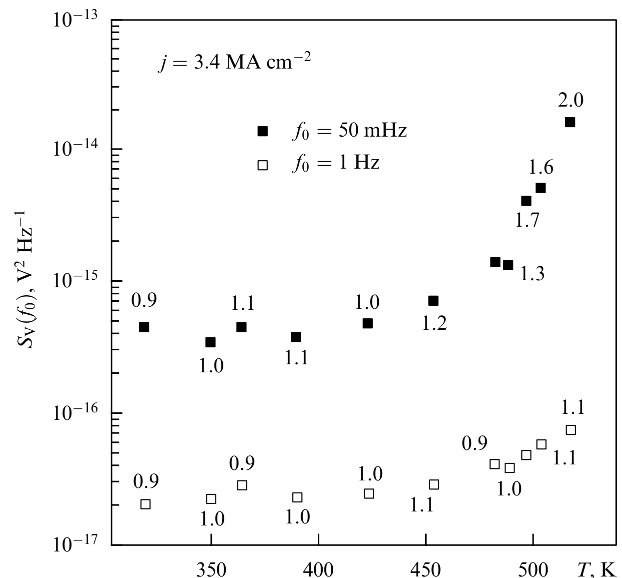

Figure 8. Temperature dependences of $1/f^2$ noise PSD at direct current $j = 3.4$ MA cm^{-2} for an Al/Si(1%) film at two frequencies $f_0 = 50$ mHz and $f_0 = 1$ Hz.

obtained from the analogous dependences for the frequency range 40–400 mHz. It follows from these results that at 1 Hz $1/f^2$ noise fails to manifest itself over the entire temperature range, whereas at 50 mHz and $T \leqslant 450$ K it is masked by the noise with a $1/f^\gamma$-like spectrum and $\gamma = 0.9-1.1$. The intensity of EM processes increases with increasing temperature, which results in a stronger EM noise. At 525 K, exponent γ equals 2 (see Fig. 8).

5.2.2 Current dependence.

At current densities $j_0 > 10^6-10^7$ A cm^{-2}, the current dependence of $1/f$ noise PSD significantly deviates from quadratic, and $1/f^2$ noise

PSD is $S_{\rm V} \propto j^n$, where exponent n takes values 3, 4, and even 7 [61]. The deviation of the current dependence of EM noise PSD from the quadratic law suggests that this noise component results from nonequilibrium fluctuations of film conduction and is linked with fluctuations of coefficients R_n in the expansion (3.2) at nonlinear CVC terms from (3.4). Conversely, at a low current density $j_0 \leqslant 10^6$ A cm^{-2}, Al films exhibit EEN with the usual quadratic dependence of PSD on the current [22, 44, 62].

Refs [12, 14, 49, 56] report dependences of $1/f^2$ noise PSD on direct current density j_0 at different temperatures in the form

$$S_{\rm V}(f) = \frac{Bj_0^3}{Tf^2} \exp\left(-\frac{E_{\rm a}}{kT}\right), \tag{5.9}$$

where B is constant and $E_{\rm a}$ is EM activation energy equal to the activation energy of the self-diffusion of metal atoms.

Dependences $S_{\rm V}(f)$ on current density j_0 at different temperatures are shown in Fig. 9 [14]. As mentioned in Section 3.2, such current dependences can arise when there is a correlation between coefficients $R_0(t)$ and $R_1(t)$ in expression (3.2), but the physical mechanism of such correlation remains to be elucidated.

At the same time, Ref. [13] documented a $S_{\rm V} \propto j^{4.3}$-like dependence at $T = 300-500$ K and current density $j_0 = (1-3) \times 10^6$ A cm^{-2} for alloy films of Al/Si/Ti(0.15%) with dimensions $l = 1.2$ μm (length), $b = 2.8$ μm (width), and $h = 1$ μm (thickness). Temperature dependences of $1/f$ noise PSD for these films had an activation nature with the activation energy $E_{\rm a} = 0.59$ eV at the current density $j = 3 \times 10^6$ A cm^{-2}. Mean γ was found to be 2.3, suggesting irreversible film damage [13].

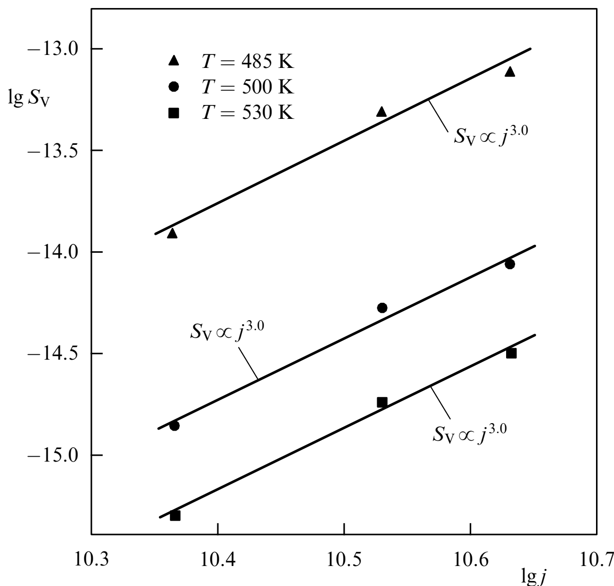

Figure 9. Plots of $1/f^2$ noise PSD vs. current density for an Al/Si(1%) film at three different temperatures [14].

5.2.3 $1/f^2$ noise in polycrystalline films. Results of certain studies indicate that the EM component of $1/f^2$ noise in polycrystalline metal films results from atomic diffusion along grain boundaries [12, 14, 50]. This inference was confirmed by experiments in which activation energy $E_{\rm a}$ determined from the temperature dependence of $1/f^2$ noise PSD was shown to correspond to the activation energy of diffusion along grain boundaries. For Al films, Neri et al. [12] found the activation energy over the temperature range $T = 327-396$ K to be 0.6 eV. In [52], the activation energy for alloy films of Al/Si(0.75%)/Cu(0.5%) with $h = 0.8$ μm and $b = 1.8$ μm fell in the range of $E_{\rm a} = 0.58-0.77$ eV.

The correspondence between activation energies of $1/f^2$ noise PSD obtained in these experiments and diffusion along grain boundaries was confirmed by Koch [63] who demonstrated that $1/f^2$ noise activation energy in films of Al and its alloys increased in parallel with the rise in the activation energy of diffusion with a growing content of impurities. Because at a low concentration of impurities (1% at.) they are largely segregated at the grain boundaries, the activation energy of self-diffusion along the boundaries increases by the amount of atom-vacancy binding energy [20]. Under these conditions, impurities do not appreciably influence the bulk properties of crystallites.

5.2.4 $1/f^2$ noise in monocrystalline films

In submicron metallic conductors having a monocrystalline or bamboo structure with the mean grain size much greater than the film width, mass transfer along grain boundaries is absent [58, 59]. Such conductors are characterized by a large activation energy $E_{\rm a}$ found from the temperature dependence of $1/f^2$ noise PSD compared with the activation energy of diffusion along grain boundaries determined in the previous section for polycrystalline films. For example, temperature dependence of $1/f^2$ noise PSD for Al films with a monocrystalline or bamboo structure (grain size $d \approx 3$ μm, $h = 0.3-0.45$ μm, $b = 0.6-0.9$ μm, and $l = 400$ μm) gave $E_{\rm a} \approx 0.8$ eV [64]. Such a value was accounted for by the activation energy of diffusion along dislocations. The activation energy of self-diffusion along dislocations in Al films measured in [65, 66] was 0.85 eV, i.e., close to that obtained in [64]. Typical measures of current density found in [64] were $j = 4 \times 10^6$ A cm^{-2}.

Submicron Al/Si(1%) conductors ($h = 0.9$ μm, $b = 0.9$ μm, $l = 1$ mm) used as connections in IMC have a bamboo structure and a mean grain size bigger than the film width, with grain boundaries perpendicular to the current flow. Their activation energy found from the temperature dependence of $1/f^2$ noise PSD was 1.45 eV [14]. This value corresponds to the activation energy of self-diffusion across the crystal lattice in bulk aluminium [20, 21]. This finding can be accounted for by the absence of mass transfer along grain boundaries in films with a bamboo structure [58, 59]. Therefore, the $1/f^2$ noise observed in the above experiments should be ascribed to atomic lattice diffusion.

Figure 10 illustrates the temperature dependence of parameter $F \sim S_{\rm V}$ in the Arrhenius coordinates at the current density $j = 3.4$ MA cm^{-2} [14]. Parameter F is defined through EM $1/f^2$ noise PSD as

$$F = S_{\rm R} \frac{kT}{\rho j},$$

where

$$S_{\rm R} = \frac{S_{\rm v}}{I_0^2} = \frac{C}{f^2} \frac{\rho j}{kT} \exp\left(-\frac{E_{\rm a}}{kT}\right).$$

Here, C is a constant depending on the film structure and sample geometry, and ρ is the resistivity of the film material.

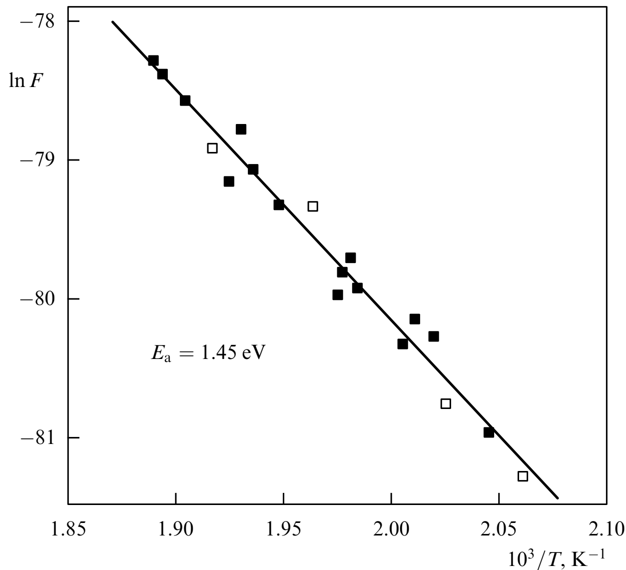

Figure 10. Temperature dependence of $F \sim S_V$, where S_V is the $1/f^2$ noise PSD, for an Al/Si(1%) film at current $j = 3.4$ MA cm^{-2} in the Arrhenius coordinates [14].

Activation energy $E_a = 1.45$ eV was derived from the slope of the straight line in Fig. 10.

5.2.5 On the formation of the $1/f^2$ spectrum. The lifetime of vacancies in a film τ_v depends on the distance between sinks L_v and is defined by relation (2.6). In a film sample having a homogeneous structure, vacancy sinks are uniformly distributed throughout the bulk. This accounts for the small dispersion of the vacancies' diffusion length L_v and constant probability of annihilation of individual vacancies in any time interval. In this case, fluctuations in film resistance will have the Debye – Lorentz spectrum with a characteristic frequency f_1 defined through the mean vacancy lifetime τ_v as $f_1 = 1/(2\pi\tau_v)$ [8].

Estimates of vacancy diffusion length L_v in [14] indicate that it lies in the range from 20 to 200 nm. Characteristic frequency f_1 in the Lorentz spectrum for these two extreme L_v values at $T = 350$ K can be determined using formula (2.6) and, assuming for lattice diffusion that $D_v \approx 10^{-24}$ m^2 s^{-1} [20, 21]:

for $L_{v1} = 20$ nm,

$$\tau_{v1} = 4 \times 10^7 \text{ s}, \quad f_1 \approx 4 \times 10^{-9} \text{ Hz};$$

for $L_{v2} = 200$ nm,

$$\tau_{v1} = 4 \times 10^9 \text{ s}, \quad f_1 \approx 4 \times 10^{-11} \text{ Hz}.$$

These estimates indicate that characteristic frequency f_1 in the Lorentz spectrum lies significantly lower than frequencies starting from which EM noise was examined in [14] (from a few milliherz). It appears that the $1/f^2$ spectrum of EM noise observed by certain authors is attributable to the appearance of noise with a very low Lorentz spectrum inflection frequency in EM processes.

5.3 NEFN due to heterogeneous inclusions

This type of NEFN was observed in molybdenum films deposited onto oxidized silicon by magnetron sputtering [27, 33, 42] at a relatively low condensation rate, facilitating the formation of thin oxide interlayers at grain boundaries [30].

5.3.1 Test samples and experimental technique. Amplitude fluctuations of zeroth, second, and third harmonics were studied in Mo films of thickness $h = 247$ nm and $h = 560$ nm deposited at condensation rates $w_c = 1$ nm s^{-1} (type 1 samples) and $w_c = 2.4$ nm s^{-1} (type 2 samples), respectively. All films had a width of 40 μm. For type 1 films, resistivity was $\rho_f = 34$ μΩ cm and temperature coefficient of resistance $\alpha_f = 0.55 \times 10^{-3}$ K^{-1}; for type 2 films, $\rho_f = 11$ μΩ cm and $\alpha_f = 2.6 \times 10^{-3}$ K^{-1}.

SDs of amplitude fluctuations of signal-response harmonics in response to sinusoidal test influence were measured as described in Section 4.2. The test signal frequency was $f_1 = 10$ kHz. SDs of amplitude fluctuations of zeroth, second, and third harmonics of the signal-response were measured over a frequency range from 10 Hz to 1 kHz. Moreover, $1/f$ noise PSD was measured at a given direct current through the sample. NEFN, induced by generation of excess vacancies due to Joule heating (see Section 5.1), was excluded by choosing direct and alternating current density below 10^4 A cm^{-2}.

5.3.2 Results of the study. Films deposited at a lower condensation rate ($w_c = 1$ nm s^{-1}) had an elevated content of reactive-gas admixtures (in the first place, oxygen) and, as a result, enhanced levels of $1/f$ noise and CVC nonlinearity defined by relation (3.4) as compared with films deposited at 2.4 nm s^{-1}. Amplitudes of the second and third harmonics measured at the fundamental frequency current $I_1 = 0.45$ mA for type 1 samples were roughly two and four orders of magnitude larger than those for type 2 samples, respectively. In molybdenum films deposited at 2.4 nm s^{-1}, the level of amplitude fluctuations of the second and third harmonics, i.e., the NEFN level, at the current density $j < 0.5 \times 10^4$ A cm^{-2} turned out to be lower than the background noise of the measuring unit and could not be measured in [27]. In contrast, type 1 samples deposited at a low condensation rate ($w_c = 1$ nm s^{-1}) exhibited high NEFN levels [27, 33].

Figure 11 shows frequency dependences of relative $1/f$ noise PSD for type 1 Mo films [33, 34]. Curve *1* obtained at a direct current $I_0 = 0.45$ mA corresponds to the total flicker-noise power, i.e., summarized PSD of EFN and NEFN in accordance with expressions (3.6) and (3.9). Curves *2*, *3*, and *4* for samples subjected to a sinusoidal current with an amplitude $I_1 = 0.45$ mA represent amplitude fluctuation SDs of zeroth, second, and third harmonics defined by expressions (4.2), (4.3), and (4.4), respectively, i.e., spectral NEFN densities of the film samples.

It can be seen from Fig. 11 that voltage fluctuation SD of the zeroth harmonic coincides, within the limits of measuring error, with amplitude fluctuation SD of the second harmonic, in agreement with expressions (4.2) and (4.3) according to which fluctuations $U_0(t)$ and $U_2(t)$ are both given by coefficient $R_1(t)$ in expansion (3.2).

The results of measurements from Ref. [33] were used to estimate the relative contribution of each term in expression (3.9) to the overall flicker noise at a frequency of 10 Hz and current $I_0 = 0.45$ mA (curve *1* in Fig. 11). It was found that the contribution of the first term (equilibrium fluctuations of resistance R_0) was 39.5%, compared with 60% of the second one (nonequilibrium fluctuations of coefficient R_1) whereas

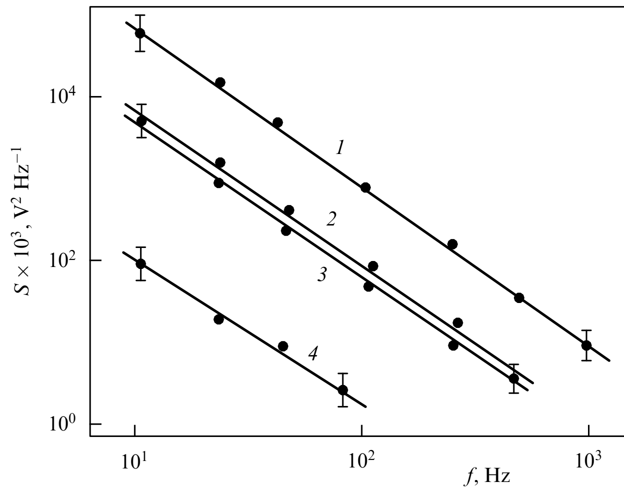

Figure 11. Frequency dependences of relative $1/f$ noise PSD for a Mo film deposited at a rate of $w_c = 1$ nm s^{-1}: curve *1* — at a direct current $I_0 = 0.45$ mA; curves *2*, *3*, and *4* — at harmonic influence with a current amplitude $I_1 = 0.45$ mA for the zeroth, second, and third harmonics, respectively [33].

the contribution of the third term fluctuations (R_2-related nonequilibrium fluctuations) was only 0.5%. In other words, the largest contribution to flicker-noise PSD was made by fluctuations of coefficient R_1 by the quadratic term in expression (3.7). The contribution of the term $R_1 I_0$ to film resistance (3.2) at current $I_0 = 0.45$ mA did not exceed 1% [33].

Figure 12 shows frequency dependences of fluctuation SD of noise amplitude modulation for the second m_1 and third m_2 harmonics (curves *1* and *2*, respectively) measured in a sinusoidal current through a sample with an amplitude $I_0 = 0.45$ mA and the frequency dependence of relative

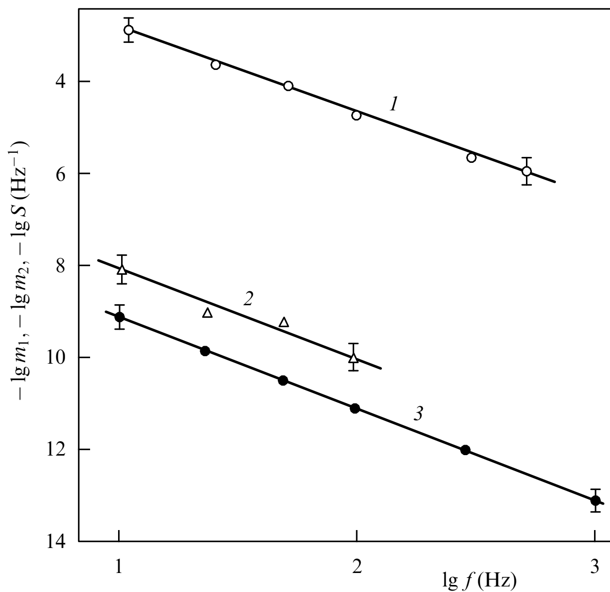

Figure 12. Frequency dependences of SD of fluctuations of the extent of noise amplitude modulation for the second m_1 and third m_2 harmonics (curves *1* and *2*, respectively) in a sinusoidal current amplitude $I_1 = 0.45$ mA and of relative flicker-noise PSD in a direct current $I_0 = I_1 = 0.45$ mA (curve *3*) for a Mo film deposited at $w_c = 1$ nm s^{-1} [27].

flicker-noise PSD S measured in a direct current $I_0 = I_1 = 0.45$ mA (curve *3*) [27]. The magnitude of noise amplitude modulation m_1 and m_2 and relative flicker-noise PSD $S(f)$ measured in a direct current are defined by the following expressions:

$$m_1 = \frac{S_{U_2}(f)}{U_2^2}\,, \quad m_2 = \frac{S_{U_3}(f)}{U_3^2}\,, \quad S(f) = \frac{S_V(f)}{V_0^2}\,.$$

Here, U_2 and U_3 are the amplitudes of the second and the third harmonics, respectively, and V_0 is constant voltage: $V_0 = I_0 R$, where R is the film resistance.

It follows from Fig. 12 that the magnitude of noise amplitude modulation of the second harmonic m_1 induced by fluctuations of coefficient R_1 in expression (3.2) (the coefficient by the quadratic term of CVC) is six orders of magnitude larger than the relative fluctuation level of constant voltage V_0 at a given direct current equal to the sinusoidal current amplitude of 0.45 mA.

One cause of quadratic nonlinearity in metal films can be the overbarrier mechanism of conduction through thin oxide interlayers at crystallite boundaries (Schottky emission) [29, 30]. In metal films showing a high affinity to oxygen, thin oxide interlayers (~ 1 nm) are likely to develop at grain boundaries due to the capture of oxygen molecules by the film in the course of condensation leading to the isolation of individual grains. This in turn results in the development of overbarrier conduction contributing to the overall conduction of the film, the appearance of CVC quadratic nonlinearity, a further increase of cubic nonlinearity, and the generation of nonequilibrium conduction fluctuations. Under these conditions, NEFN is manifest as fluctuations of coefficients R_1 and R_2 in expression (3.2).

As shown in [27], the dependence of the second harmonic amplitude U_2 on the test signal voltage amplitude U_1 plotted in coordinates $\{\lg U_2, U_1^{0.5}\}$ is linear for the films included in the study. This suggests that the observed CVC nonlinearity is indeed due to the overbarrier emission current [30] while fluctuations of coefficient R_1 in (3.2) are most probably related to fluctuations of potential barrier heights at grain boundaries. Modulation of the potential barrier heights is believed to be involved in the development of $1/f$ noise in many physical systems, e.g., in MIS structures during tunnel transport of carriers through a dielectric [67, 68].

These experimental findings indicate that the development of NEFN in Mo films deposited at a low condensation rate is due to heterogeneous inclusions in the bulk of the film in the form of thin oxide interlayers at grain boundaries that support nonmetallic (activation) conduction mechanisms.

6. Nonequilibrium flicker noise in thin-film contacts

6.1 Test samples for separating flicker noise in film contacts measured in direct current

It should be borne in mind that flicker noise of a film resistor measured at a given direct current is determined by the intrinsic noise of the film and contacts with it. Each of these $1/f$ noise sources may be either equilibrium or nonequilibrium and of different magnitude.

In Ref. [13], the bulk noise of a resistive Ni/Cr layer and the noise of Al contacts were separated by using two types of samples having resistive layers of different length l (l_1 and l_2)

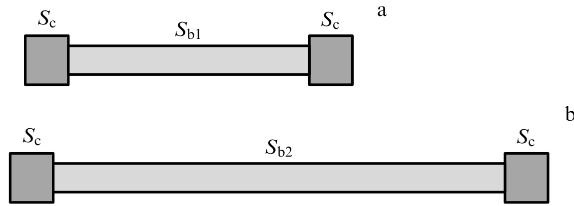

Figure 13. Resistors with different film square numbers designed to separate contact and film noises [13].

but an identical thickness h and width b of the conducting film (different square numbers $n_{\square} = l/b$) with two contact surfaces S_c (Fig. 13). Measurements of $1/f$ noise PSD S_{V1} and S_{V2} for the two types of samples at the same current were used to calculate $1/f$ noise PSD of a single film contact S_c and $1/f$ noise PSD in one square of the conducting layer S_b based on expressions [13]

$$S_{V1} = S_{b1} + 2S_c\,, \qquad S_{V2} = S_{b2} + 2S_c\,, \tag{6.1}$$

where S_{b1} and S_{b2} are defined through the square numbers of film samples $n_{\square 1} = l_1/b_1$ and $n_{\square 2} = l_2/b_2$, with $n_{\square 1}$ and $n_{\square 2}$ being film square numbers in Figs 13a and 13b, respectively. Also, $S_{b1} = n_{\square 1} S_b$ and $S_{b2} = n_{\square 2} S_b$.

The results of $1/f$ noise PSD S_{V1} and S_{V2} measurements were used to find noise PSD of resistive film S_b and contact S_c from formula (6.1). By employing test structures depicted in Fig. 13, it was possible to distinguish the noise of the resistive Ni/Cr layer and Al contacts [13]. It was shown that the FN profile of film contacts was similar to that of strictly $1/f$ noise; its level depended on the current but was independent of the resistance of the layer.

Usually, the noise of a single contact is smaller than that of the resistor (e.g., it was less than 10% for Ni/Cr resistors with Al contacts in [13]). Therefore, it can not be always measured with the use of the test structures shown in Fig. 13. In such cases, a special test structure is fabricated for measuring S_c with a sufficiently large number N of identical serial-connected film contacts, and its noises are compared with the noises of a homogeneous film of the same material and length but having only two contacts [69].

In Ref. [31], contact noises were separated using the test structure schematically represented in Fig. 14. Resistors (a) and (b) were placed on one substrate but had different square numbers n_1 and n_2 and contained two and four film contacts, respectively.

Let us use the following notation: S_{V1} and S_{V2} for noise PSD in the structures depicted in Figs 14a and 14b, respectively; S_c for noise PSD of a single contact in resistors at the same current densities through the contact at $b = \text{const}$; N_1, N_2 for contact numbers in the structures in Figs 14a and 14b, respectively; S_{b1} for $1/f$ noise PSD in one square of the resistive film for structures (a) and (b) at identical current densities; n_1 and n_2 for the square numbers of the resistive film in structures (a) and (b) ($n_1 = a_1/b, n_2 = 2a_2/b$); and t_1 and t_2 for the contact number to square number ratio in structures (a) and (b) ($t_1 = N_1/n_1,\ t_2 = N_2/n_2$). In the general case, assuming the absence of a correlation between excess noises in the resistive film and contacts for structures with N_1 and N_2, there is a system of equations for noise PSD in resistive structures:

$$S_{V1} = N_1 S_c + n_1 S_{b1}\,, \qquad S_{V2} = N_2 S_c + n_2 S_{b1}\,. \tag{6.2}$$

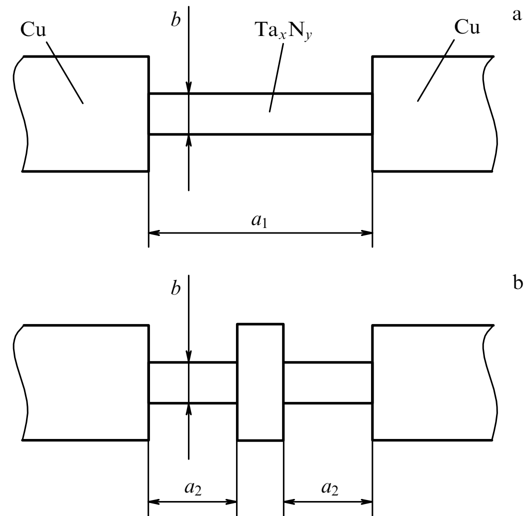

Figure 14. Resistors with different numbers of film squares and contacts designed to separate contact and resistive film noises [31].

Solution of (6.2) for S_c and S_{b1} yields the following expressions for noise PSD of a single contact:

$$S_c = \frac{n_1 S_{V2} - n_2 S_{V1}}{n_1 n_2 (t_2 - t_1)} \tag{6.3}$$

and for noise PSD of one square of the resistive film,

$$S_{b1} = \frac{N_1 S_{V2} - N_2 S_{V1}}{n_1 n_2 (t_1 - t_2)}\,. \tag{6.4}$$

It has been shown in studies [31, 40] using the test structures of Fig. 14 that $1/f$ noise levels in tantalum film contacts of resistors manufactured by different technologies differ by more than four orders of magnitude. In such metal contacts, FN is not significantly stronger than in the resistor only if both are produced in one technological circuit, i.e., without depressurizing of the vacuum chamber after the deposition of the resistive layer.

6.2 Results of investigations into nonequilibrium flicker noise and nonlinearity of CVC in film contacts of resistors

The contribution of contacts to CVC nonlinearity and $1/f$ noise PSD was evaluated using commercial tantalum nitride thin-layer resistors [31, 40, 70, 71]. CVC nonlinearity of the contacts was determined by measuring amplitudes of the second and third harmonics of the signal-response under harmonic test influence [70] or by measuring voltage fluctuations of the constant component U_C of the sample's signal-response produced by the excitation of the film sample by a rectangular current pulse train [71] (see Sections 4.2 and 4.3).

NEFN in contacts was examined in [31, 40] over the frequency range from 20 Hz to 1 kHz by measuring the SD of voltage fluctuations of the constant component U_C in a film resistor subjected to rectangular current pulses of varying amplitude V_p with period $T = 8$ μs and duration $t_p = 1$ μs. The measuring error did not exceed 20%. Moreover, $1/f$ noise PSD was measured at direct current I_0. $1/f$ noise at current I_0 was compared with that at the pulsed current. For measuring noise PSD, the constant voltage on the resistor $V_0 = RI_0$ (R is

the sample resistance) was chosen to equal the pulse amplitude, i.e., $V_0 = V_p$.

6.2.1 Description of test resistors. For the study of NEFN development mechanisms in resistive layers and contacts, $1/f$ noise was examined in thin-layer resistors obtained by different methods of film deposition and contact formation. The samples studied are briefly described below.

Resistive films were fabricated by magnetron sputtering of a tantalum target onto glass ceramics in an argon-nitrogen (10%) mixture at various deposition rates [30]. In all cases, equal gas pressure was maintained at $(7-10) \times 10^{-2}$ Pa. The deposition rate was modulated by varying voltage on the target, with simultaneous monitoring of its ion current I_{ion}. The substrate temperature during the deposition of the resistive layer was chosen to be 350 °C.

The study included thin-film resistors of four types. Regardless of the type, resistive films of all samples had surface resistivity of $100 \pm 10\ \Omega\,\square^{-1}$. Contacts with the resistive layer were formed from copper films of width $h_{\text{Cu}} = 1$ μm with a chromium sublayer (for better adhesion). Metallic layers were deposited by the thermal evaporation technique in a vacuum under residual gas pressure in the chamber below 7×10^{-4} Pa.

Samples of types 1 and 2 differed in terms of deposition rates of the resistive layer. The deposition lasted 6 min 40 s at the current $I_{\text{ion}} = 1.5$ A through the target for type 1 samples (high deposition rate) and 52 min at $I_{\text{ion}} = 0.3$ A for type 2 samples (low deposition rate).

In samples of types 3 and 4, conditions for the formation of the resistive film were chosen to be identical and ensured the lowest flicker-noise level [72]. For this purpose, a two-layer structure was fabricated in which the resistive film was formed in two stages, that is, the first layer was deposited for 9 min at the current 1.2 A and the second one for 10 min at $I_{\text{ion}} = 0.3$ A.

A distinctive feature of type 4 samples was the formation of both the resistive layer and the contacts in one technological circuit without depressurizing the vacuum chamber, that is, the film deposition was followed within 3 min by the deposition of the chromium sublayer and then of the copper layer.

The copper layer being formed, samples of all types were annealed in a vacuum at 350 °C for 30 min to stabilize their structure [73] and reduce the $1/f$ noise level. After that, copper, nickel, and gold layers of thicknesses $h_{\text{Cu}} = 5$ μm, $h_{\text{Ni}} = 0.5$ μm, and $h_{\text{Au}} = 2$ μm, respectively, were successfully deposited by electrodeposition technology.

The test structures shown in Fig. 14 were used to evaluate the contribution of contacts to CVC nonlinearity of resistors and separate contact $1/f$ noise from the total noise power of the resistors. The film square number in structures (a) and (b) was $n_1 = 25$ and $n_2 = 10$, respectively. The geometric size of the samples was as follows: length $a_1 = 2500$ μm and $a_2 = 500$ μm, width $b = 100$ μm.

6.2.2 Experimental results. Figure 15 shows frequency dependences of $1/f$ noise PSD for one square of the resistive layer S_b in four types of resistors; $1/f$ noise PSD values for a single film contact S_c at frequency $f = 130$ Hz and at direct current $I_0 = 6$ mA are presented in the table.

It can be seen from Fig. 15 that the highest $1/f$ noise level occurred in type one samples in which the resistive layer was obtained at a high deposition rate. In these structures, NEFN

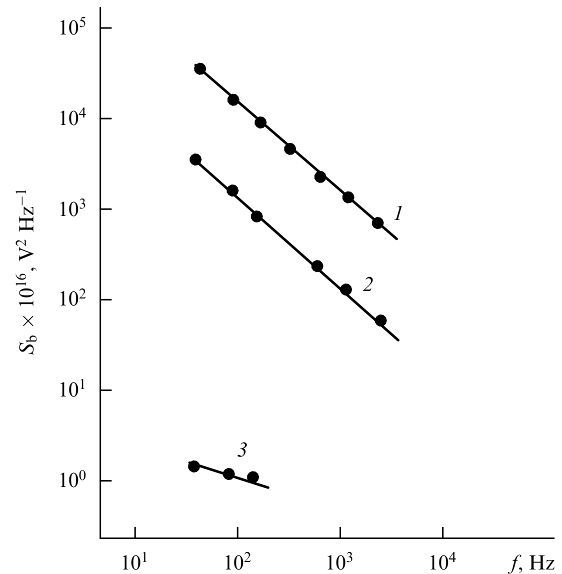

Figure 15. Frequency dependences of $1/f$ noise PSD in Ta_xN_y films. Curve *1* — for type 1 samples, curve *2* — for type 2 samples, curve *3* — for types 3 and 4 samples [31]; $I_0 = 6$ mA.

of the contacts was comparable with that of the resistive film (see the table).

Table. $1/f$ noise PSD values for a single film contact of Ta film-based resistors at frequency $f = 130$ Hz and direct current $I_0 = 6$ mA [40].

Sample type	1	2	3	4
$S_c \times 10^{16}$, V^2 Hz^{-1}	3500	< 100	4	0.32

It follows from the table that $1/f$ noise PSD of type 1 film contacts was more than 10^4 times higher than that of type 4 samples. Depending on manufacturing technology, the contribution of contact $1/f$ noise to the total resistor noise was either comparable with the FN level of the resistive film or exceeded it. However, the contact $1/f$ noise in high-quality film resistors was negligible compared with the noise level in the resistive film.

In type 2 structures with the resistive layer formed by the low-rate deposition technique, the contact $1/f$ noise proved to be significantly weaker than the noise of the resistive film and could not be separated by measuring at direct current in the test structures shown in Fig. 14. For this reason, nonequilibrium $1/f^{\gamma}$ noise in the contacts in type 2 samples was studied in Ref. [40] under pulse test influence. The results of $1/f$ noise measurements under pulse influence were compared with flicker-noise measurements in a direct current with voltage $V_0 = V_p = 5$ V on the sample.

Studies [31, 40] revealed significant difference between EFN and NEFN levels for type 2 film resistors. Specifically, equilibrium FN PSD measured at a frequency of 10 Hz and constant voltage $V_0 = 5$ V was more than 1000 times higher than nonequilibrium FN PSD measured at pulse voltage with amplitude $V_p = V_0 = 5$ V. At $V_0 \leqslant 5$ V, the contribution of nonequilibrium fluctuations in contact conduction to the total FN of the resistor was insignificant. At the same time, relative SD of voltage fluctuations of the constant component $S_N = S_U/U_C^2$ at 10 Hz (NEFN) was three orders of

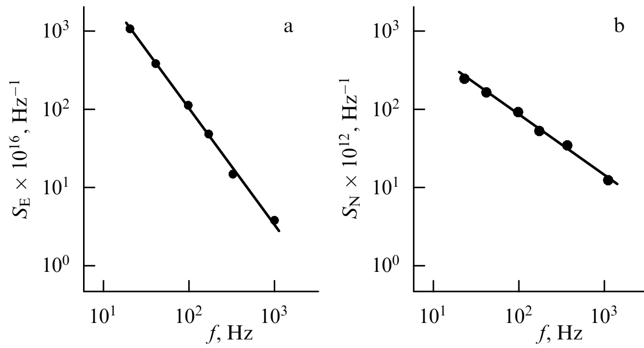

Figure 16. Frequency dependences of equilibrium $1/f$ noise PSD S_E measured in direct current (a) and of nonequilibrium $1/f^{\gamma}$ noise PSD S_N measured under pulse test influence (b) for type 2 Ta_xN_y samples [31].

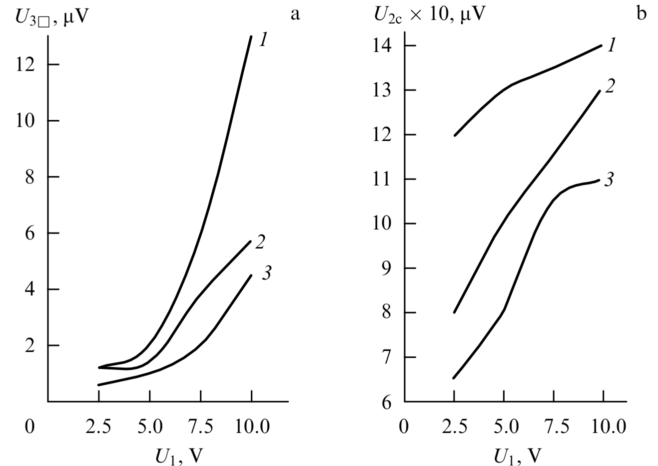

Figure 17. Plots of the amplitudes of the third harmonic of the signal-response of one square of resistive film (a) and of the second harmonic of the signal-response of the contact site (b) versus test-signal amplitude: curve *1* — type 1 samples (high deposition rate), curve *2* — type 2 samples (low deposition rate), curve *3* — type 4 samples (two-step deposition) [70].

magnitude higher than the relative SD of EFN $S_E = S_V/V_0^2$ measured in direct current (Fig. 16), indicating a high degree of noise amplitude modulation of constant voltage component U_C.

It follows from Fig. 16b that nonequilibrium $1/f$ noise PSD of the contacts shows frequency dependence in accordance with the $1/f^{\gamma}$ law with the spectrum shape exponent $\gamma = 0.7 - 0.9$, whereas for the EFN spectrum measured in direct current, the exponent $\gamma = 1 - 1.2$ [31, 34].

The above results suggest a different physical nature of the mechanisms of EFN produced at a given direct current through the resistive film (when the contribution of the NEFN component at $V_0 \leqslant 5$ V is negligibly small) and of NEFN generated upon the excitation of the sample by a sequence of rectangular current pulses (voltage fluctuations of the constant component).

At a relatively small density of direct current through the sample ($j_0 < 10^5$ A cm^{-2}), the EFN level in a resistive film is largely determined by equilibrium resistance fluctuations, i.e., the term $R_0(t)$ in the expression for CVC (3.4). Voltage fluctuations of the constant component (NEFN) are related to fluctuations of the nonlinear part of resistance $N(I, t)$ in the expression for CVC (3.4) and especially to fluctuations of the coefficient $R_1(t)$ in expansion (3.2). Coefficient R_1 gives quadratic nonlinearity of CVC resulting from contact nonlinearity as demonstrated experimentally in Refs [70, 71].

CCV components created by the nonlinearity of the contacts and the resistive layer were separated in Ref. [71]. It turned out that in type 2 samples the main contribution to CCV, hence to resistor NEFN, was made by resistive film contacts. CVC nonlinearity of the same resistors was studied in Ref. [70] by the method of harmonic test influence on the sample (see Section 4.2). The test structures depicted in Fig. 14 were used to separate components of cubic and quadratic nonlinearity of CVC in the resistive layer and contacts from the total resistor nonlinearity. It was found that the resistive layer was largely characterized by cubic CVC nonlinearity, whereas quadratic nonlinearity predominates in the contacts.

Figure 17 shows plots of the amplitudes of the third harmonic of the signal-response for one square of the resistive film (a) and of the second harmonic of the signal-response of contact unit (b) versus test-signal voltage U_1 for different types of resistors [70]. The highest levels of nonlinearity (Fig. 17a) and $1/f$ noise (see Fig. 15) were characteristic of the resistive layer obtained by the high rate deposition technique (type 1 samples). The physical mechanism of cubic CVC nonlinearity of the resistive layer in type 1 samples is supposed to be associated with the creation and annihilation of vacancies [8]. This suggestion is confirmed by the experimentally observed high levels of $1/f$ noise and voltage of the third harmonic of the signal-response in these samples and lower levels of these parameters in type 2 samples fabricated at a small deposition rate of the resistive layer. During its condensation on the substrate in type 1 samples obtained at a high deposition rate, vacancies have no time to emerge at the condensation front on the film surface (because of the low diffusion speed) and prove to be bricked up in the bulk of the condensate [74]. In the course of aging and exploitation of the resistor, these vacancies tend to coalesce, giving rise to micropores and cavities near which current density is enhanced. Concurrently formed local overheating zones are the sites of subsequent film destruction.

Levels of contact unit nonlinearity with respect to the second harmonic in the samples under study are also significantly different over the entire range of test-signal voltage U_1 (Fig. 17b). The CVC nonlinearity level of the contacts in the second harmonic is the most sensitive parameter that characterizes contact site quality [70]. Contact of type 1 resistors obtained at a high condensation rate exhibit the highest levels of both nonlinearity and $1/f$ noise.

As the fundamental frequency voltage on the resistor grows, the amplitudes of the second and third harmonics increase. As shown in [70], when the first harmonic amplitude $U_1 = 10$ V, the levels of the second and the third harmonics of the contact's signal response are greater by more than a factor of ten than the level of nonlinearity of a single square in the resistive film for all types of samples studied. The contribution of the contact transient resistance to the structure's total resistance for one square of the resistive film is less than 0.5%. In other words, at a relatively high current, contacts can make a significant contribution to quadratic and cubic CVC nonlinearity and NEFN, despite their relatively small contribution to resistor resistance.

6.2.3 Temperature dependence. Ref. [75] reports measurements of $1/f$ noise PSD in tantalum thin-film resistors over

the temperature range from 300 to 400 K at a given direct current through the sample (EFN) and of spectral density of voltage fluctuations of the constant component under pulse influence on the sample at $V_p = V_0 = 5$ V (NEFN). The EFN level has been shown to increase and NEFN to decrease with rising temperature. The decrease of NEFN is attributable to the lowering of transient resistance of film contacts with a rise in temperature while the increase of EFN with temperature to the activation of mobile defects in the crystal lattice (vacancies) of the resistive film (see Section 2.2). These results indicate that the mechanisms of EFN and NEFN generation in thin-film resistors and film contacts are of different physical natures.

6.2.4 Effect of annealing on the 1/f noise in film contacts. The effect of annealing on FN in Ti–Al and V–Al thin-film contacts was investigated in Ref. [76]. The condensation temperature was chosen to be 390 K. Further annealing was performed at 520 K for 15 min. Prior to the annealing, $\gamma = 2-3$ for contact FN compared with $\gamma = 1-1.2$ for homogeneous titanium and vanadium films. After the annealing, γ for Me1–Me2 film contacts became close to unity. Enhanced γ values for untreated contacts suggest the presence of a nonequilibrium $1/f^{\gamma}$ noise component related to the elevated concentration of excess vacancies in the contact unit area.

6.2.5 Physical mechanisms of NEFN generation in film contacts. The appearance of NEFN in film contacts of the resistive layer-Me or Me1–Me2 is first and foremost related to the properties of interfaces, specifically to gas adsorption and subsequent oxidation of the interface between conducting layers during the manufacturing and storage of the resistor.

One of the possible causes of CVC nonlinearity and NEFN in contacts may be the overbarrier or tunnel mechanism of conduction [29, 30] through a thin oxide layer formed at the interface between conducting layers. The overbarrier and tunnel mechanisms of conduction are responsible for the appearance of quadratic and the increase of cubic CVC nonlinearities and for NEFN generation. The NEFN mechanism in film contacts may be due to fluctuations in the height of the potential barrier at the interface between conducting layers during the overbarrier or tunnel transport of carriers. In the case of low-quality contacts, this type of fluctuations may play a decisive role in generating resistor NEFN. When the resistive layer and contacts are deposited in one technological circuit, no oxide interlayer is formed at the resistive layer-metal film interface. Under these conditions, quadratic and cubic nonlinearity levels, as well as NEFN of the contacts, are at their lowest.

Besides NEFN produced by the mechanisms of overbarrier and tunnel emission, film contacts also exhibit NEFN induced by the creation and annihilation of excess vacancies in the contact zone (see Section 5.1).

7. Nonequilibrium flicker noise due to thermodynamic nonequilibrium of film structure and external influences

This type of NEFN arises in conducting films of different materials when their crystalline structure is not in thermodynamic equilibrium (e.g., in freshly fabricated films) or was disequilibrated by an external impact (e.g., deformation or irradiation). The presence of unstable defects in a film leads to its instability. Its structure becomes regular with time under the effect of ambient temperature or electrical current that cause the free energy of the film-substrate system to fall. During this process, the number of defects in the film decreases in compliance with the exponential law [73] leading to a slow irreversible reduction in film resistance and generation of NEFN. In the general case, this noise is a nonstationary one. The relaxation time of the process varies in a very broad range. The effect of an electrical load or elevated temperature on the conducting film results in a decreased relaxation time and more rapid stabilization of film resistance. A change of resistance R by ΔR for a certain time t determines an important film characteristic, its stability $\Delta R/R$.

Stability of film elements is sometimes enhanced by means of artificial aging under effect of thermal treatment (annealing) in a vacuum or in the atmosphere of an inert gas at a temperature of 550–650 K, i.e., much higher than working temperatures. After the annealing, the film structure becomes stable in time because thermal fluctuations of the lattice at room temperature can not substantially shift the defects that escaped annealing at a higher temperature. This accounts for a lower $1/f$ noise level (usually EFN) in annealed films.

For NEFN associated with a thermodynamically nonequilibrium structure, exponent γ specifying the shape of the spectrum is as a rule high and may reach $\gamma \approx 2-3$.

7.1 NEFN caused by natural aging and annealing of metal films

Time-dependent changes of $1/f$ noise PSD in naturally aging Al films obtained at room temperature $T_c = 300$ K were studied in Refs [45, 77]. Similar studies of Cr films deposited onto glass ceramics at a condensation temperature $T_c = 400$ K are reported in Refs [78, 79] and at an optimal temperature $T_c = 470$ K ensuring the lowest $1/f$ noise level in Ref. [80]. In all these cases, $1/f$ noise PSD exponentially decreased with time, with a time constant τ_0 characteristic of the annealing of structural point microdefects [73]. For example, for Al films, $\tau_0 = 5$ min [77], and practically all defects with the low activation energy were annealed for 30 min. Annealing of nonequilibrium structural defects in a metal film resulted in a high level of nonstationary NEFN.

Aging of Cr films was accompanied by a decrease of γ [78]. Measurements taken immediately after the fabrication of Cr films gave $\gamma = 2.5-3$. It decreased to 0.7–1.2 within 30–45 min after placing the samples in a vacuum (NEFN energy spectrum in Ref. [78] was measured during time $t \ll \tau_{rel}$, where τ_{rel} is the NEFN relaxation time). Higher γ values characterized more nonequilibrium condensates with a higher concentration of excess vacancies.

It has been shown in Ref. [78] that the $1/f$ noise level in aging chromium films decreases in parallel with a reduction of intrinsic mechanical stresses and resistivity. The lowering of macrostresses in the course of annealing chromium films suggests that the condensate's specific volume in these samples increases due to coalescence of vacancies into complexes or closed micro- and submicropores. Because the micropore volume equals the sum of atomic volumes, and the volume of the same number of isolated vacancies is roughly two times smaller, the condensate's specific volume increases, leading to weaker mechanical stresses [74].

The results of aging and annealing studied on metal films indicate that they contain mobile defects with different

activation energies annealed at different temperatures and during different time periods. Annealing of films at temperatures higher than the condensation temperature causes an abatement of FN due to a reduced concentration of excess vacancies or other defects in the bulk of the condensate. Defects contributing to FN in metal and alloy films were identified in [66]. They proved to be vacancies and dislocations. Annealing resulted in a quasi-equilibrium concentration of microdefects that persisted in time or changed very slowly at temperatures below the annealing temperature. $1/f$ noise in annealed metal films was either stationary or quasi-stationary. Low current density was associated with EFN.

7.2 Radiation-induced NEFN in metal films

Metal films subjected to irradiation develop additional nonequilibrium structural defects. Such defects may spontaneously disappear from the crystal lattice during the subsequent storage of the films. The relaxation time for defects with low and high activation energies is a few minutes and many months, respectively. Annealing at an elevated temperature results in a faster removal of defects from the crystal lattice and generation of nonstationary NEFN.

Studies [81, 82] concerned effects of annealing-induced defects on $1/f$ noise PSD in Al films over a temperature range from 10 to 300 K. The defects were created by irradiating the films with fast electrons of energy 1 MeV and fluence 3.7×10^{23} e/m^2 at 10 K. The irradiated samples experienced a six-fold rise in the noise level and a 25% increase in resistance. Isochronic annealing of the samples for 600 s, with the temperature gradually rising from 10 to 300 K, resulted in the recovery of the initial $1/f$ noise level and resistance at 200 K. The authors' explanation of this finding is that annealing decreased the number of mobile defects in the films irradiated with fast electrons.

Film irradiation induces defects with different activation energies, hence with different annealing temperatures. Based on the Dutta – Horn model [5], the authors of Ref. [82] received the distribution function for the activation energy of defects $D(E_a)$ in irradiated and unirradiated samples. For the latter, the distribution function $D(E_a)$ had its largest value in an energy range of approximately 0.2 – 0.9 eV. These defects were associated with the development of EFN in the films. Following irradiation and subsequent annealing at 105 K, the function $D(E_a)$ proved to be uniform over an energy range from hundredths of electron volts to 0.15 eV. The annealing temperature of induced defects in Al films with such a low activation energy was below 200 K. These defects were responsible for NEFN in a temperature range between 10 K and 100 K.

Results similar to those in Refs [81, 82] were received by Pelz and Clarke [83] in a study concerned with the effect of induced defects on nonequilibrium $1/f$ noise PSD in copper films.

The effect of γ-radiation on the $1/f$ noise level in niobium films was evaluated in Ref. [45]. Noise PSD was possible to measure at room temperature because the activation energy of induced microdefects in Nb films was higher than in Al [82] or Cu [83] films. Studies reported in Ref. [45] demonstrated a rise in the $1/f$ noise level following irradiation of Nb films due to the development of additional defects in the crystal lattice (Fig. 18, curve *2*). After the current-induced annealing of the sample, the $1/f$ noise magnitude decreased to approximately that in the unirradiated sample (curve *3*) even though it remained slightly higher than the initial NF (curve *1*) due to

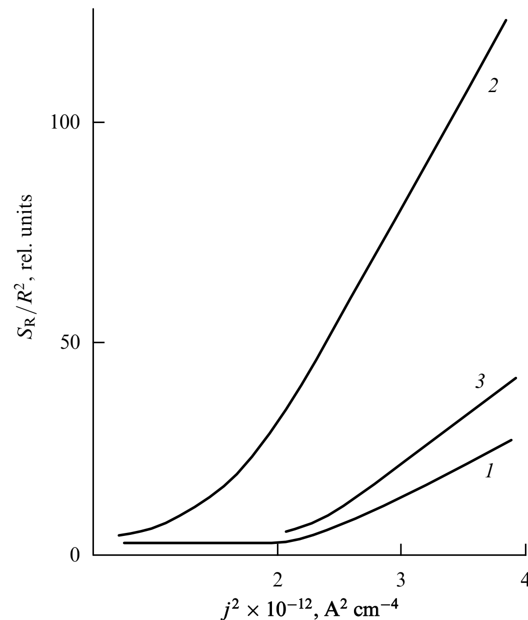

Figure 18. Plots of relative $1/f$ noise SD versus direct current density for niobium films: curve *1* — for the initial unirradiated sample, curve *2* — for the same sample following irradiation, curve *3* — after current-induced annealing of the sample [45].

the persistence of additional radiation-induced structural microdefects.

To summarize, irradiation of metal films with high-energy particles gives rise to a nonequilibrium nonstationary $1/f$ noise component in their FN associated with excessive induced microstructural defects (largely vacancies and dislocations [66]), the level of which depends on their concentration, while NEFN relaxation time is determined by the activation energy of the induced defects.

7.3 Strain-induced NEFN in conductors

Of special interest are direct experiments designed to study the effects of controlled mechanical stresses caused by external forces on the level and characteristics of $1/f$ noise in metal films because such stresses may be conducive to the development of nonequilibrium $1/f^\gamma$ noise.

Fleetwood and Giordano observed a rise of about a factor of ten in $1/f$ noise upon deformation of platinum, gold, silver, lead, and tin films deposited onto glass and elastic substrates [84]. Removal of the external strain caused noise relaxation to smaller levels for a period of a few hours to several months, although the resulting noise magnitude remained higher than the initial one (prior to deformation). The authors ascribed the observed experimental effects to the creation and annihilation of structural microdefects. It may be supposed that film samples in these experiments underwent plastic deformation. Also, it was shown in Ref. [84] that $1/f$ noise in films on elastic substrates was less stable than in films on glass. It should be noted that mechanical stresses applied to the films on elastic substrates in the above experiments were stronger than those on glass.

Quantitative studies of the effect of externally induced controlled mechanical stresses on the $1/f$ noise levels and characteristics in metal films were carried out in [78, 79, 85]. Used in [78, 79] were chromium films on glass and in [85] aluminium films on a PM-1 elastic polyimide substrate.

Tensile and compressive stresses were generated in chromium films by bending a console-fixed substrate [8, 78, 79]. Tensile stress developed when the external bending force was applied to the free end of the substrate perpendicular to its plane from the side occupied by the deposited film. The same force was applied from the opposite side to raise the compressive stress. Displacement of the unfixed end of the substrate with the film was used as a measure of the relative deformation and for calculating the mechanical stress in the elastic strain region by Hooke's formula.

Figure 19 shows frequency dependences of $1/f$ noise PSD for a chromium film at different mechanical stresses in the elastic strain region [78]. Curve *1* corresponds to internal mechanical stresses $\sigma_0 = 10^8$ Pa (in the absence of an external force). Increasing mean tensile stress from $\sigma = \sigma_0 = 10^8$ Pa to $\sigma = 3 \times 10^8$ Pa causes an approximate 1000-fold reversible rise in the magnitude of $1/f$ noise PSD at 10 Hz while the exponent γ increases from 1 to 2.5. The removal of the external bending force results in the recovery of $1/f^\gamma$ noise PSD in the elastic strain region to its initial level depicted by curve *1* in Fig. 19, without the application of an external force. Film resistance in this strain region also undergoes a reversible 0.5–1% increase. In films with a relative deformation $\varepsilon \geqslant 0.4\%$ in the elastic strain region, irreversible changes of both FN level and resistance occur [79].

It should be borne in mind that the bending of the console-fixed film-coated substrate creates a mechanical stress gradient along the film, giving rise to a vacancy level gradient. The resultant diffuse flux of vacancies along the mechanical stress gradient promotes stress relaxation and, consequently, a decrease in the film's free energy [58, 59]. This can probably account for such a large increase of the NEFN level and exponent γ with increasing mechanical stress for the Cr films studied in Ref. [78].

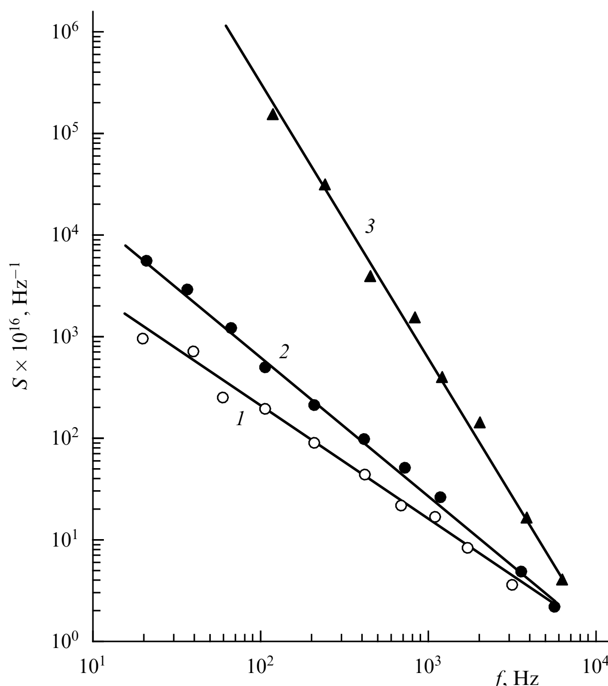

Figure 19. Effect of mechanical stress on $1/f$ noise PSD in chromium films; $h = 80$ nm, $T = 300$ K: line *1* — $\sigma = \sigma_0 = 10^8$ Pa; line *2* — $\sigma = 2 \times 10^8$ Pa; line *3* — $\sigma = 3 \times 10^8$ Pa [78].

In Al films on an elastic polyimide substrate, there was also an approximate 30-fold increase in the $1/f$ noise PSD at 20 Hz with increasing (from 0 to 1.2×10^8 Pa) tensile mechanical stresses created by an external tensile force and uniformly distributed along the film length [85]. Simultaneously, the exponent γ increased over the same mechanical stress range from 1.1 to 1.7.

It should be noted that an enhanced internal mechanical stress in aluminium and chromium films manufactured by different technologies also leads to a rise in the $1/f$ noise PSD level and the exponent γ [86, 87].

Interesting results were obtained by subjecting metal conductors to heat cycles [14]. Specifically, thermocycles induced sharp (several microohms) microfluctuations in the sample's resistance. This phenomenon, termed resistance fluctuations in Ref. [14], appears to be associated with the creation and annihilation of dislocations due to the high heat-induced thermal stress level in the film as a result of dissimilar coefficients of linear thermal expansion of film and substrate materials [30].

Study [88] is focused on the effect of mechanical stresses created by an external tensile force on $1/f$ noise in carbon fibers 6 µm in diameter and 10 cm in length and having a resistance of 41.3 kΩ. The fibres were subjected to a variety of deforming stresses, from elastic to plastic strains. $1/f$ noise PSD was found to increase approximately 20-fold upon a rise in tensile stress from 0 to 2.5×10^{10} Pa, whereas the fiber resistance increased only by a few percent. The removal of the stress resulted in a four-fold rise in the FN level above the initial one. This irreversible change in the FN magnitude was in all probability due to plastic deformation of the crystal lattice in carbon fibers.

To conclude, the foregoing experimental results indicate that mechanical stresses induced by an external force in metal films and other conductors give rise to nonequilibrium $1/f^\gamma$ noise related to an elevated concentration of nonequilibrium defects, e.g., vacancies, in metals. In the elastic strain region, this NEFN may be stationary, provided the nonequilibrium defect level in the film remains constant in time. Nonuniform mechanical stresses along the conducting film produce a high NEFN level due to vacancy diffusion along the mechanical stress gradient.

8. Nondestructive quality control of film conductors, resistors, and contacts by measuring flicker noise

8.1 Forecasting electromigration stability of thin films from $1/f$ noise

In Ref. [89], a method was proposed to forecast stability of thin Al films experiencing EM damage based on the evaluation of equilibrium $1/f$ noise generated by the vacancy mechanism. The method arose from the results of an experiment that showed an enhanced $1/f$ noise in fine-grained Al films [62]. Specifically, an approximate two-fold decrease in the mean grain size brought about an increase in the $1/f$ noise level by three orders of magnitude; comparison of grain size distribution curves revealed that this increase was associated with the rise in the relative number of small grains ($d_{av} \leqslant 50$ nm). Also, it was known that [58] the median time to a failure due to EM for fine-grained Al films was smaller than that for coarse-grained ones. Based on this knowledge, the authors of Ref. [89] used measure-

ments of equilibrium $1/f$ noise PSD to assess the EM stability of metal films.

Equilibrium FN PSD displays activation temperature dependence with the activation energy equaling the vacancy formation energy E_v (see Section 2.2), which can be found from the temperature dependence of $1/f$ noise PSD. However, the median time to failure t_{50} of thin-layer conductors tested for EM stability is defined by the relation [58, 59]

$$t_{50} = A j^{-n} \exp\left(\frac{E_a}{kT}\right), \tag{8.1}$$

where proportionality coefficient A is a conductor's characteristic depending on the film material, structure, and geometry. Exponent $n = 1$ at small current densities $j \leqslant 10^5$ A cm^{-2} and increases with them, usually taking values from 1 to 5 [59].

It is known [20, 21] that the vacancy mechanism of diffusion plays the key role in metals, and the activation energy of self-diffusion E_a in expression (8.1) is the sum of the activation energies involved in vacancy formation E_v and migration E_m, i.e.,

$$E_a = E_v + E_m\,.$$

The activation energy of atomic self-diffusion E_a decreases in parallel with the vacancy formation energy E_v. Simultaneously, the $1/f$ noise level increases in accordance with (2.7) and (2.8). Energy E_v in fine-grained films is smaller than in coarse-grained ones, which means a lower activation energy E_a for the former. It is this fact that allows EM stability of metal films to be evaluated from the EFN level.

However, EFN measurements can not be used to estimate the activation energy of self-diffusion of metallic atoms E_a, which enters expression (8.1) for the median time to failure t_{50}. Moreover, such measurements prove unsuitable for forecasting EM stability of high-quality metal films with a low concentration of mobile defects. These films exhibit, at a relatively low current density, equilibrium $1/f$ noise arising from fluctuations in the mobility of charge carriers upon electron scattering by acoustic phonons as described by the Hooge formula (2.1).

Many works published to date have exposed the relationship between the EM stability of thin metal films and nonequilibrium $1/f^2$ noise levels [12–14, 44, 60]. The results reported are sometimes different because the film samples used in these studies have different properties. Nevertheless, these works reveal certain common features. The observed relationship between the median time to failure and the EM $1/f^2$ noise level is due to the enhanced $1/f^2$ noise in samples with a higher density of defects that act as vacancy sources (sinks) [20] and therefore modulate EM stability of the films [58, 59]. Chen and colleagues [90] confirmed in direct experiments that Al films with an elevated excess noise have a smaller median time to failure. Also, Neri et al [12] used temperature dependences of nonequilibrium EM $1/f^2$ noise to calculate the activation energy for Al films and found it to be 0.67 eV. It corresponded to the activation energy of vacancy diffusion along grain boundaries and fell in the range of values obtained by different methods.

In experiments like those described in the preceding paragraph [12–14], measurements are made at high current and temperature loads to ensure that nonequilibrium $1/f^2$ noise PSD exceeds the total FN of a film sample at a given direct current. Measurements in direct current usually give nonequilibrium $1/f^2$ noise PSD higher than equilibrium $1/f$ noise PSD (for which the exponent $\gamma \approx 1$) only at very low frequencies (on the order from a few milliherz to one herz).

For this reason, the methods described in Section 4 can be recommended for EM $1/f^2$ noise studies since they permit the separation of nonequilibrium $1/f^2$ noise from the total noise power. When a method based on the measurement of amplitude fluctuation spectra of signal-response harmonics is employed, sinusoidal influence on the sample is sometimes given along with high-density direct current [91]. In the modern production of electronic devices and IMC, preference should be given to pulse test influence on the sample [31] as the technically simplest method.

In any case, results of nonequilibrium $1/f^2$ noise PSD measurement can be used for early detection of EM damages to thin-film conductors when other methods are inefficient [12, 66].

8.2 Quality control of film resistors based on 1/*f* noise

Today, FN measurements are used to predict the quality and reliability of passive components of various electronic devices and IMC, such as thin-layer conductors, contacts, and film resistors. Analysis of published works indicates that in many cases NEFN is by far the most informative quality parameter compared with EFN, although this fact is not as a rule specified. It is nonequilibrium (nonlinear) fluctuations that carry information about disturbances in the crystal lattice of solids and exhibit high sensitivity to latent defects.

By way of example, Sikula et al. [46, 92] undertook diagnosis of various electronic devices by measuring low-frequency noise with special reference to quality evaluation and prediction of reliability of Ag/Pd and Ag paste-based thick films from the FN level [46]. The authors report the existence of a fundamental FN component having a strictly $1/f$ spectrum for which PSD $S \propto I_0^2$ and an excess noise component with the $1/f^{\gamma}$ spectrum generated by defects. For the samples with an excess noise component, exponent $\gamma \approx 1.4$ is used to detect structural imperfections in conducting films. This component is supposed to be NEFN.

At the same time, EFN produced in the course of creation and annihilation of vacancies in metals is sometimes used to evaluate not only EM stability of thin-layer conductors (see the previous section) but also stability of contact systems and film resistors. In the general case, however, EFN measurements are insufficient to exercise nondestructive quality control of IMC passive elements and evaluate their reliability. Figure 20 illustrates a change in the $1/f$ noise energy spectrum for two Ni/Cr resistors subjected to annealing at current $I_0 = 3$ mA and $T = 520$ K for 420 h [13]. It can be seen that resistors R_1 and R_2 had similar $1/f$ noise levels prior to annealing. Afterwards, $1/f$ noise in resistor R_1 increased by two orders of magnitude and the resistance drift was 4%; $1/f$ noise in resistor R_2 remained unaltered while the resistance drift was less than 0.5%. These data suggest that annealing resulted in serious damage to resistor R_1 although its $1/f$ noise was initially identical to that of resistor R_2. This study failed to forecast the stability of resistor R_1 from measurements of $1/f$ noise PSD prior to the annealing. It may be supposed that the study measured the equilibrium $1/f$ noise of resistors R_1 and R_2, which carries no information about their quality.

Quality control of various electronic devices and passive elements of IMC can be exercised simultaneously based on CVC nonlinearity parameters and the $1/f$ noise level. For

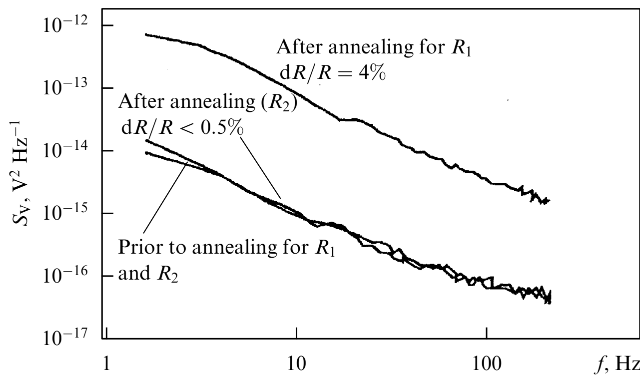

Figure 20. Changes of relative $1/f$ noise PSD for two Ni/Cr film resistors after annealing at $T = 520$ K for 420 h [13].

example, stability of Ag/Pd and Ag paste-based thick-film resistors was evaluated from the level of $1/f$ fluctuations of conduction and from the amplitude of the third harmonic of the signal response. Generally speaking, diagnosis of electronic devices is possible based on parameters of quadratic, cubic, and higher nonlinearities of CVC, and also on NEFN levels, because all of them carry information about different forms of latent defects in the crystal lattice of solid bodies.

8.3 New principles of flicker-noise spectroscopy.
The works of Timashev [94, 95] offer new possibilities for obtaining information based on the analysis of chaotic time series of dynamic variables that characterize evolution of complex nonlinear systems (including natural ones) by means of computer processing of previously digitized signals. This method, known as flicker-noise spectroscopy (FNS), is equally suitable for the analysis of electrical noises in various physical systems. It consists of attaching informative importance to distinguishable irregularities (bursts, jumps, breaks of derivatives of varying order) of dynamic variables. The high informational value of FNS is due to the fact that properties of each type of irregularity in any system indicative of FN character and level can be deduced not only from the analysis of noise PSD but also from the analysis of diverse moments of various orders. For chaotic signals, 'passport parameters' derived from the comparison of general phenomenological dependences and experimental data are introduced. FNS can be used for the analysis of both stationary and nonstationary random processes. The method was verified by the analysis of dynamics of various physico-chemical processes, e.g., voltage fluctuations in electrochemical systems, and by the studies of solar activity fluctuations [96, 97]. Unfortunately, there are still no publications on the use of FNS for FN studies in conducting films, resistors, contacts, and semiconductors.

9. Conclusions

Nonequilibrium flicker noise (NEFN) in conducting films and contacts is closely related to nonlinear conduction mechanisms. While equilibrium flicker noise (EFN) is associated with fluctuations of resistance entering Ohm's law (coefficient by the linear CVC term), fluctuations of coefficients by nonlinear CVC terms produce nonequilibrium $1/f^{\gamma}$ noise and can make the largest contribution to the total $1/f$ noise power at high current density. Both the level and the characteristics of these fluctuations in concrete cases depend on the mechanisms of charge carrier transport and dispersion.

Metal and alloy films have different mechanisms of NEFN generation. Manifestation of individual mechanisms depends on the film sample microstructure, measuring conditions (current strength, temperature), and external influences (deformation, irradiation, etc.). Metal films often exhibit EFN with a $1/f$-like spectrum and nonequilibrium electromigration noise with a $1/f^2$ spectrum simultaneously, but the latter is in many cases manifested only at high current loads and relatively low frequencies (fractions of a herz).

A variety of experimentally observed dependences of flicker-noise PSD on current density, temperature, and frequency are attributable to the difference in relative EFN and NEFN contributions to the total noise power of the sample. In metal films containing heterogeneous inclusions in the form of thin dielectric layers along grain boundaries due to an elevated content of gas contaminants, the contribution of fluctuations of coefficients at nonlinear CVC terms to the $1/f$ noise level can predominate even at a relatively small current density across the sample $j < 10^4$ A cm^{-2}. The results of $1/f$ noise studies in thin-film tantalum resistors indicate that the main contribution to resistor NEFN is made by contacts, while their contribution to resistance is insignificant.

Both the degree of CVC nonlinearity and the nonequilibrium $1/f^{\gamma}$ noise level carry information about latent defects and damages in the crystal lattice of solid bodies. The main types of defects responsible for CVC nonlinearity and NEFN in conducting films and contacts include excess vacancies, dislocations, various heterogeneous inclusions, such as dielectric layers at the contact surface or in the bulk of the film, local mechanical stresses, pores, and cracks, responsible for the nonuniform film heating by the current. This makes the degree of CVC nonlinearity and the nonequilibrium $1/f^{\gamma}$ noise level informative quality parameters of conducting films and contacts.

Methods for the study of nonequilibrium conduction fluctuations in two-terminal networks with weak nonlinearity described in the present review permit us to separate NEFN from the total $1/f$ noise power (the method for measuring amplitude fluctuation spectra of signal-response harmonics under harmonic test influence on a sample and the method for measuring voltage fluctuations of the constant component of the sample's signal-response under pulse test influence). The method for measuring NEFN in noninertial two-pole devices under pulse test influence is highly sensitive to latent defects. The methods described in the review may be recommended for the study of fluctuation phenomena in different types of passive noninertial two-terminal networks in physical, physico-chemical, and biological systems.

With further improvement of IMC quality and manufacturing technologies for up-to-date electronic devices, the amount of latent defects in these articles decreases. Therefore, traditional methods of nondestructive quality control and prediction of reliability of various types of electronic appliances, even with the use of such an informative and sensitive to latent defects parameter as $1/f$ noise measured routinely at a given direct current through the sample, become inefficient. Equilibrium flicker noise measurements can be used for this purpose only in some cases. But it is only NEFN that carries information about latent defects in conducting films and contacts and can serve as a valuable

indicator of their quality. NEFN can be used for nondestructive quality control in the modern production of conducting and resistive films, contacts, interlayer transitions (vias) and other structural elements of electronic devices and IMC.

At the same time, NEFN in conducting films and contacts remains poorly known. No physical and mathematical models have been proposed for the different types of NEFN considered in this review, and its statistical properties remain to be elucidated. Therefore, new methods to investigate NEFN are needed, in addition to those described in the review, for experimental studies of nonequilibrium flicker fluctuations in conducting films (and traditional methods of noise PSD measurement in direct current). One of them is the aforementioned flicker-noise spectroscopy (FNS) that measures not only noise PSD but also diverse moments of various orders. It is hoped that the application of this method to the studies of nonequilibrium $1/f^{\gamma}$ noise in conducting films and contacts will yield new data about its nature in these systems and in solids at large.

References

1. Johnson J B *Phys. Rev.* **26** 71 (1925)
2. Schottky W *Phys. Rev.* **28** 74 (1926)
3. Bochkov G N, Kuzovlev Yu E *Usp. Fiz. Nauk* **141** 151 (1983) [*Sov. Phys. Usp.* **26** 829 (1983)]
4. Hooge F N, Kleinpenning T G M, Vandamme L K J *Rep. Prog. Phys.* **44** 479 (1981)
5. Dutta P, Horn P M *Rev. Mod. Phys.* **53** 497 (1981)
6. Kogan Sh M *Usp. Fiz. Nauk* **145** 285 (1985) [*Sov. Phys. Usp.* **28** 170 (1985)]
7. Weissman M B *Rev. Mod. Phys.* **60** 537 (1988)
8. Zhigal'skiĭ G P *Usp. Fiz. Nauk* **167** 623 (1997) [*Phys. Usp.* **40** 599 (1997)]
9. Hooge F N *IEEE Trans. Electron Dev.* **ED-41** 1926 (1994)
10. Voss R F, Clarke J *Phys. Rev. Lett.* **36** 42 (1976)
11. Gulyaev A M, Kukoev I V, Miroshnikova I N, in *Materialy Dokladov Mezhdunarodnogo Nauchno-Tekhnicheskogo Seminara "Shumovye i Degradatsionnye Protsessy v Poluprovodnikovykh Priborakh"* ("Noise and Degradation Processes in Semiconductor Devices". Proc. Intern. Scientific and Technical Workshop) (Moscow: MNTORES, 2001) p. 21
12. Neri B, Diligenti A, Bagnoli P E *IEEE Trans. Electron Dev.* **ED-34** 2317 (1987)
13. Touboul A, Verdier F, Herve Y, in *Noise in Physical Systems and 1/f Fluctuations*: *Proc. of the Intern. Conf., Kyoto, Japan, 1991* (Eds T Musha, S Sato, M Yamamoto) (Tokyo: Ohmsha, 1992) p. 73
14. Neri B, Ciofi C, Dattilo V *IEEE Trans. Electron Dev.* **ED-44** 1454 (1997)
15. Hooge F N, Hoppenbrouwers A M H *Physica* **45** 386 (1969)
16. Hooge F N *Physica B + C* **83** 14 (1976)
17. Hooge F N, in *Noise in Physical Systems and 1/f Fluctuations*: *Proc. of the 14th Intern. Conf., Leuven, Belgium, 14–18 July, 1997* (Eds C Claeys, E Simoen) (Singapore: World Scientific, 1997) p. 3
18. Giordano N *Rev. Solid State Sci.* **3** 27 (1989)
19. Musha T, in *Proc. of the 15th Intern. Conf. on Noise in Physical Systems and 1/f Fluctuations, Hong Kong, Aug. 23–26, 1999* (Ed. C Surya) (Hong Kong: Polytechnic Univ., 1999) p. 18
20. Bokshteĭn B S *Diffuziya v Metallakh* (Diffusion in Metals) (Moscow: Metallurgiya, 1978)
21. Girifalco L A *Statistical Physics of Materials* (New York: Wiley, 1973) [Translated into Russian (Moscow: Mir, 1975)]
22. Potemkin V V, Bakshi I S, Zhigal'skiĭ G P *Radiotekh. Elektron.* **28** 221 (1983) [*Radio Eng. Electron. Phys.* **28** 89 (1983)]
23. Van der Ziel A *Fluctuation Phenomena in Semi-Conductors* (New York: Academic Press, 1959) [Translated into Russian (Moscow: IL, 1961)]
24. Buckingham M J *Noise in Electronic Devices and Systems* (Chichester: E. Horwood, 1983) [Translated into Russian (Moscow: Mir, 1986)]
25. Zhigal'skiĭ G P *Pis'ma Zh. Eksp. Teor. Fiz.* **54** 510 (1991) [*JETP Lett.* **54** 513 (1991)]
26. Zhigalskii G P, in *Noise in Physical Systems and 1/f Fluctuations*: *Proc. of the Intern. Conf., Kyoto, Japan, 1991* (Eds T Musha, S Sato, M Yamamoto) (Tokyo: Ohmsha, 1992) p. 39
27. Zhigal'skiĭ G P *Zh. Fiz. Khim.* **69** 1355 (1995)
28. Zhigal'skii G P, Jones B K, in *Proc. of the 15th Intern. Conf. on Noise in Physical Systems and 1/f Fluctuations, Hong Kong, Aug. 23–26, 1999* (Ed. C Surya) (Hong Kong: Polytechnic Univ., 1999) p. 172
29. Chopra K L *Thin Film Phenomena* (New York: McGraw-Hill, 1969) [Translated into Russian (Moscow: Mir, 1972)]
30. Zhigal'skiĭ G P, Jones B K *Fizicheskie Yavleniya v Tonkikh Metallicheskikh Plenkakh* (The Physical Properties of Thin Metal Films) (Moscow: Izd. MIET, 1996) [Translated into English (London: Taylor & Francis, 2003)]
31. Zhigal'skiĭ G P, Karev A V *Radiotekh. Elektron.* **44** 222 (1999) [*J. Commun. Technol. El.* **44** 206 (1999)]
32. Kirbi P L *Electron. Eng.* **37** 722 (1965)
33. Zhigal'skii G P, in *Fluctuation Phenomena in Physical Systems*: *Proc. of the 7th Vilnius Conf., Palanga, Lithuania, 4–7 Oct., 1994* (Ed. V Palenskis) (Vilnius: Vilnius Univ. Press, 1994) p. 285
34. Jones B K, Zhigal'skii G P, in *Noise in Physical Systems and 1/f Fluctuations*: *ICNF 2001*: *Proc. of the 16th Intern. Conf., Gainesville, Florida, USA, 22–25 Oct. 2001* (Ed. G Bosman) (River Edge, NJ: World Scientific, 2001) p. 73
35. Lorteije J H J, Hoppenbrouwers A M H *Philips Res. Rep.* **26** 29 (1971)
36. Jones B K, Francis J D *J. Phys. D: Appl. Phys.* **8** 1172 (1975)
37. Palenskis V P, Leont'ev G E, Mikolaĭtis G S *Radiotekh. Elektron.* **21** 2433 (1976)
38. Jones B K *Electron. Lett.* **12** 110 (1976)
39. Malakhov A N *Fluktuatsii v Avtokolebatel'nykh Sistemakh* (Fluctuations in Self-Oscillatory Systems) (Moscow: Nauka, 1968)
40. Zhigal'skiĭ G P, Karev A V *Oboronnyĭ Kompleks — Nauchno-Tekhnicheskomu Progressu Rossii* (3–4) 50 (1997)
41. Thompson M W *Defects and Radiation Damage in Metals* (London: Cambridge Univ. Press, 1969) [Translated into Russian (Moscow: Nauka, 1983)]
42. Zhigal'skiĭ G P, in *Materialy Dokladov Mezhdunarodnogo Nauchno-Tekhnicheskogo Seminara "Shumovye i Degradatsionnye Protsessy v Poluprovodnikovykh Priborakh"* ("Noise and Degradation Processes in Semiconductor Devices". Proc. Intern. Scientific and Technical Workshop) (Moscow: MNTORES, 2001) p. 152
43. Dul'nev G N, Semyashkin E M *Teploobmen v Radioelektronnykh Apparatakh* (Heat Exchange in Radio Electronic Devices) (Leningrad: Energiya, 1968)
44. Schwarz J A et al. *J. Appl. Phys.* **70** 1561 (1991)
45. Potemkin V V, Stepanov A V, Zhigal'skii G P, in *Noise in Physical Systems and 1/f Fluctuations* (AIP Conf. Proc., Vol. 285, Eds P H Handel, A L Chung) (New York: American Institute of Physics, 1993) p. 61
46. Sikula J, Touboul A, in *Noise in Physical Systems and 1/f Fluctuations* (AIP Conf. Proc., Vol. 285, Eds P H Handel, A L Chung) (New York: American Institute of Physics, 1993) p. 206
47. Bagnoli P E et al. *J. Appl. Phys.* **63** 1448 (1988)
48. Neri B et al., in *Noise in Physical Systems*: *Including 1/f Noise, Biological Systems and Membranes*: *Proc. of the 10th Intern. Conf., Aug. 21–25, 1989, Budapest, Hungary* (Ed. A Ambrózy) (Budapest: Akadémiai Kiadó, 1990) p. 237
49. Chen T M, Fang P, Cottle J G, in *Noise in Physical Systems*: *Including 1/f Noise, Biological Systems and Membranes*: *Proc. of the 10th Intern. Conf., Aug. 21–25, 1989, Budapest, Hungary* (Ed. A Ambrózy) (Budapest: Akadémiai Kiadó, 1990) p. 515
50. Smith R G, Biery G A, Rodbell K P *Appl. Phys. Lett.* **65** 315 (1994)
51. Chen T M, in *Noise in Physical Systems and 1/f Fluctuations* (AIP Conf. Proc., Vol. 285, Eds P H Handel, A L Chung) (New York: American Institute of Physics, 1993) p. 17
52. Yassine A M, Chen T M, in *Proc. of the 13th Conf.* "*Noise in Physical Systems and 1/f Fluctuations*" (Eds V Bareikis, R Katilius) (Singapore: World Scientific, 1995) p. 614
53. Ciofi C, Diligenti A, Neri B, in *Proc. of the 13th Conf.* "*Noise in Physical Systems and 1/f Fluctuations*" (Eds V Bareikis, R Katilius) (Singapore: World Scientific, 1995) p. 618

54. Diligenti A et al. *IEEE Electron Dev. Lett.* **EDL-6** 606 (1985)
55. Celik-Butler Z, in *Noise in Physical Systems and 1/f Fluctuations* (AIP Conf. Proc., Vol. 285, Eds P H Handel, A L Chung) (New York: American Institute of Physics, 1993) p. 200
56. Chen T M, in *Noise in Physical Systems and 1/f Fluctuations* (AIP Conf. Proc., Vol. 285, Eds P H Handel, A L Chung) (New York: American Institute of Physics, 1993) p. 17
57. Yassine A M, Chen C T-M *IEEE Trans. Electron Dev.* **ED-44** 180 (1997)
58. D'Erl F, Rosenberg R, in *Physics of Thin Films: Advances in Research and Development* Vol. 7 (Eds G Hass, M Francombe, R Hoffman) (New York: Academic Press, 1973) [Translated into Russian (Moscow: Mir, 1977) p. 284]
59. Poate J M, Tu K N, Mayer J W (Eds) *Thin Films. Interdiffusion and Reactions* (New York: Wiley, 1978) [Translated into Russian (Moscow: Mir, 1982)]
60. Dagge K et al., in *Noise in Physical Systems and 1/f Fluctuations* (AIP Conf. Proc., Vol. 285, Eds P H Handel, A L Chung) (New York: American Institute of Physics, 1993) p. 603
61. Jones B K *Adv. Electron. El. Phys.* **87** 201 (1994)
62. Zhigal'skiĭ G P, Bakshi I S *Radiotekh. Elektron.* **25** 771 (1980) [*Radio Eng. Electron. Phys.* **25** 61 (1980)]
63. Koch R H, Lloyd J R, Cronin J *Phys. Rev. Lett.* **55** 2487 (1985)
64. Ochs E et al., in *Noise in Physical Systems and 1/f Fluctuations: Proc. of the 14th Intern. Conf., Leuven, Belgium, 14–18 July, 1997* (Eds C Claeys, E Simoen) (Singapore: World Scientific, 1997) p. 415
65. Volin T E, Lie K H, Balluffi R W *Acta Metall.* **19** 263 (1971)
66. Seeger A, Stoll H, in *Proc. of the 15th Intern. Conf. on Noise in Physical Systems and 1/f Fluctuations, Hong Kong, Aug. 23–26, 1999* (Ed. C Surya) (Hong Kong: Polytechnic Univ., 1999) p. 162
67. Neri B, Olivo P, Riccò B *Appl. Phys. Lett.* **51** 2167 (1987)
68. Zhigal'skiĭ G P *Radiotekh. Elektron.* **44** 1413 (1999) [*J. Commun. Technol. El.* **44** 1301 (1999)]
69. Smirnov V I, Mata F Yu *Teoriya Konstruktsiĭ Kontaktov v Elektronnoĭ Apparature* (The Theory of Contact Constructions in Electronic Devices) (Moscow: Sovetskoe Radio, 1974)
70. Zhigal'skiĭ G P, Zaĭtsev V V *Izv. Vyssh. Uchebn. Zaved. Elektronika* (5) 79 (1997)
71. Osokin N E *Izv. Vyssh. Uchebn. Zaved. Elektronika* (1–2) 119 (1999)
72. Zhigal'skiĭ G P, Karev A V, Kosenko V E *Elektronnaya Tekhnika. Ser. 6. Materialy* (1) 70 (1992)
73. Holland L (Ed.) *Thin Film Microelectronics* (London: Wiley, 1965) [Translated into Russian (Moscow: Mir, 1968)]
74. Palatnik L S, Fuks M Ya, Kosevich V M *Mekhanizm Obrazovaniya i Struktura Kondensirovannykh Plenok* (Mechanism of Fabrication and Structure of Condensed Films) (Moscow: Nauka, 1972)
75. Zhigal'skii G P, Karev A V, in *Proc. of the 13th Conf. "Noise in Physical Systems and 1/f Fluctuations"* (Eds V Bareikis, R Katilius) (Singapore: World Scientific, 1995) p. 323
76. Zhil'kov E A et al., in *Poluprovodnikovye Pribory i Integral'nye Skhemy* (Semiconductor Devices and Integrated Circuits) (Sbornik Nauchnykh Trudov po Problemam Mikroelektroniki (Collected Works on Microelectronics), Issue 27, Ed. A A Orlikovskiĭ) (Moscow: MIET, 1976) p. 127
77. Potemkin V V et al., in *Fluctuation Phenomena in Physical Systems: Proc. of the 6th Sci. Conf., Sept. 23–27, 1991, Palanga, Lithuania* (Ed. V Palenskis) (Vilnius: Vilnius Univ. Press, 1991) p. 79
78. Zhigal'skiĭ G P, Kurov G A, Siranashvili I Sh *Izv. Vyssh. Uchebn. Zaved. Radiofiz.* **26** 207 (1983) [*Radiophys. Quantum Electron.* **26** 162 (1983)]
79. Kurov G A, Zhigal'skiĭ G P, Siranashvili I Sh, in *Puti Povysheniya Stabil'nosti i Nadezhnosti Mikroelementov i Mikroskhem. Materialy 2-go Vsesoyuz. Nauchno-Tekhnicheskogo Seminara* (Approaches to Improving Stability and Reliability of Microelements and Microcircuits. Proc. 2nd All-Union Scientific and Technical Workshop) (Ryazan': Izd. RRTI, 1982) p. 41
80. Zhigal'skiĭ G P, Fedorov A S *Izv. Vyssh. Uchebn. Zaved. Radiofiz.* **28** 1192 (1985) [*Radiophys. Quantum Electron.* **28** 831 (1985)]
81. Briggmann J et al., in *Noise in Physical Systems and 1/f Fluctuations* (AIP Conf. Proc., Vol. 285, Eds P H Handel, A L Chung) (New York: American Institute of Physics, 1993) p. 607
82. Dagge K et al., in *Proc. of the 13th Conf. "Noise in Physical Systems and 1/f Fluctuations"* (Eds V Bareikis, R Katilius) (Singapore: World Scientific, 1995) p. 603
83. Pelz J, Clarke J *Phys. Rev. Lett.* **55** 738 (1985)
84. Fleetwood D M, Giordano N *Phys. Rev. B* **28** 3625 (1983)
85. Zhigal'skiĭ G P, Sokov Yu E, Tomson N G, in *Fizika Poluprovodnikov i Mikroelektronika* (Physics of Semiconductors and Microelectronics) (Ryazan': Izd. RRTI, 1977) p. 63
86. Zhigal'skii G P, in *Noise in Physical Systems and 1/f Fluctuations* (AIP Conf. Proc., Vol. 285, Eds P H Handel, A L Chung) (New York: American Institute of Physics, 1993) p. 81
87. Zhigal'skiĭ G P, Sokov Yu E, Tomson N G *Radiotekh. Elektron.* **24** 410 (1979) [*Radio Eng. Electron. Phys.* **24** 137 (1979)]
88. Akabane H, Agu M, in *Noise in Physical Systems and 1/f Fluctuations: ICNF 2001: Proc. of the 16th Intern. Conf., Gainesville, Florida, USA, 22–25 Oct. 2001* (Ed. G Bosman) (River Edge, NJ: World Scientific, 2001) p. 99
89. Potemkin V V, Bakshi I S, Zhigal'skiĭ G P, in *Elektrofluktuatsionnaya Diagnostika Materialov i Izdeliĭ Elektronnoĭ Tekhniki* (Electrofluctuation Diagnosis of Electronic Devices) (Moscow: Izd. TsNIIITEI, 1981) p. 52
90. Chen T M, Djeu T P, Moore R D, in *Proc. on Reliability Physics, Orlando, 1985* (New York: IEEE Publ., 1985) p. 87
91. Jones B K, Xu Y Z *Microelectron. Reliab.* **33** 1829 (1993)
92. Sikula J et al., in *Proc. of the 15th Intern. Conf. on Noise in Physical Systems and 1/f Fluctuations, Hong Kong, Aug. 23–26, 1999* (Ed. C Surya) (Hong Kong: Polytechnic Univ., 1999) p. 154
93. Sedlakova V et al., in *Noise in Physical Systems and 1/f Fluctuations: ICNF 2001: Proc. of the 16th Intern. Conf., Gainesville, Florida, USA, 22–25 Oct. 2001* (Ed. G Bosman) (River Edge, NJ: World Scientific, 2001) p. 747
94. Timashev S F, in *Noise in Physical Systems and 1/f Fluctuations: ICNF 2001: Proc. of the 16th Intern. Conf., Gainesville, Florida, USA, 22–25 Oct. 2001* (Ed. G Bosman) (River Edge, NJ: World Scientific, 2001) p. 775
95. Timashev S F *Zh. Fiz. Khim.* **75** 1900 (2001) [*Russ. J. Phys. Chem.* **75** 1742 (2001)]
96. Parkhutik V P, Timashev S F *Elektrokhimiya* **36** 1378 (2000) [*Russ. J. Electrochem.* **36** 1221 (2000)]
97. Kostuchenko G T, Timashev S F, in *Chaotic Universe* (Advanced Ser. in Astrophys. and Cosmology, Vol. 10, Eds V G Gurzadyan, R Ruffini) (Singapore: World Scientific, 2000) p. 579